QCD Phase Diagrams via a Nonperturbative Approach

Yu-xin Liu
Dept. Phys., Peking Univ., China

Outline

1st Symposium on iHIC, Tsinghua University, April 8-10, 2018

I. Introduction

Strong int. matter evolution in early universe can be attributed to QCD Phase Transitions

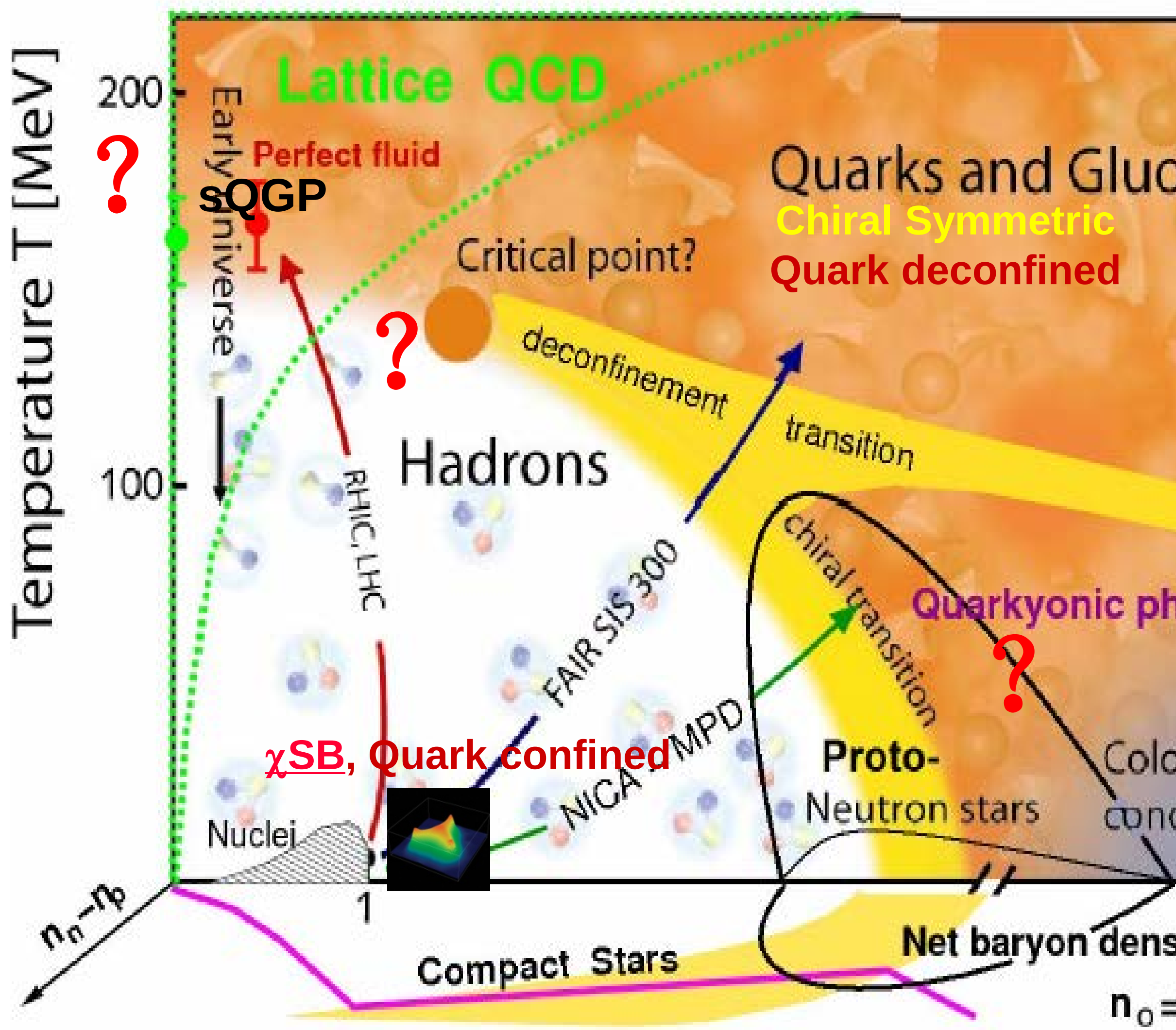

Phase Transitions involved:

Flavor Sym. – F.S. Breaking

Deconfinement–confinement

DCS – DCSB

Items Influencing the Phase Transitions:

Medium: Temperature T ,

Density ρ (or μ)

Size

Intrinsic: Current mass,

Coupling Strength,

Color-flavor structu

… …

♠ The existence of the CEP and its location have been a key subject in the QCD PT

- (p)NJL model & others give quite large μ_E^q/T_E (> 3.0)

  Sasaki, et al., PRD 77, 034024 (2008); 82, 076003 (2010); 82, 116004 (1010);
  Costa, et al., PRD 77, 096001 (‘08); EPL 86, 31001 (‘09); PRD 81, 016007(‘10);
  Fu & Liu, PRD 77, 014006 (2008); Ciminale, et al., PRD 77, 054023 (2008);
  Fukushima, PRD 77, 114028 (2008); Kashiwa, et al., PLB 662, 26 (2008);

- Lattice QCD gives smaller μ_E^q/T_E (0.4 ~ 1.1)

  Fodor, et al., JHEP 4, 050 (2004); Gavai, et al., PRD 71, 114014 (2005);
  Gupta, arXiv:~0909.4630[nucl-ex]; Li, et al., PRD 84, 071503 (2011);
  Gupta, et al., Science 332, 1525 (2011); PRD 90, 034001 (2014); ······

- DSE Calculations with different techniques generate different results for the μ_E^q/T_E (0.0, 1.1 ~ 1.3, 1.4 ~ 1.6,)

  Blaschke, et al, PLB 425, 232 (1998); He, et al., PRD 79, 036001 (2009);
  Fischer, et al., PLB 702, 438 (‘11); PLB 718, 1036 (‘13); etc,
  Qin, Liu, et al., PRL 106, 172301(‘11); PRD 90, 034022; PRD 94, 076009; etc.

- Main physics focus of current and planed facilities; Annual International Conference on this topic; etc.

♠ General requirement for the methods used in studying QCD phase transitions

- should involve simultaneously the properties of the DCSB & its Restoration, the Confinement & Deconfinement ;
- should be nonperturbative QCD approach, since the two kind PTs happen at NP QCD energy scale (10^2 MeV).

♠ Theoretical Approaches:

Two kinds - Continuum & Discrete (lattice)

Theory The Frontiers of Nuclear Science A LONG RANGE PLAN December 2007

The primary goal of the RHIC scientific program in the coming years is to progress from qualitative statements to rigorous quantitative conclusions. Quantitative conclusions require sophisticated modeling of relativistic heavy-ion collisions and rigorous comparison of such models with

Thus, an essential requirement for the field as a whole is strong support for the ongoing theoretical studies of QCD matter, including finite temperature and finite baryon density lattice QCD studies and phenomenological modeling, and an increase of funding to support new initiatives enabled by experimental and theoretical breakthroughs. The success of this effort mandates significant additional investment in theoretical resources in terms of focused collaborative initiatives, both programmatic and community oriented.

♠ **Lattice QCD:**

Running coupling behavior,
Vacuum Structure,
Temperature effect,
"Small chemical potential";
…

♠ **Continuum:**

(1) **Phenomenological models**
(p)NJL、(p)QMC、QMF、

(2) **Field Theoretical**
Chiral perturbation,
Functional RG,
QCD sum rules,
Instanton(liquid) model,

- **Dyson-Schwinger equations can play the role of a continuum approach.**

II. Dyson-Schwinger Equations — A Nonperturbative QCD Approach

(1) Outline of the DS Equations

Slavnov-Taylor Identity

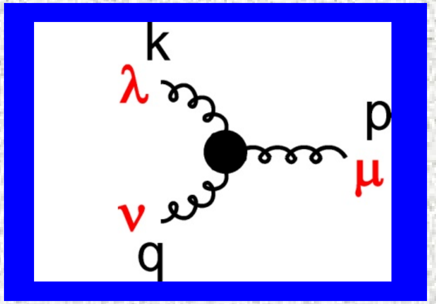

axial gauges BBZ

$$k_\lambda \, \Gamma^{\lambda\mu\nu}(k,p,q) \;=\; \Pi^{\mu\nu}(p) \;-\; \Pi^{\mu\nu}(q)$$

covariant gauges

$$k_\lambda \, \Gamma^{\lambda\mu\nu}(k,p,q) \;=\; H(k^2) \; G_{\mu,\sigma}(q,-k)\, \Pi^T_{\sigma,\nu}(p) \;-\; G_{\nu\sigma}(p,-k)\, \Pi^T_{\sigma\mu}(q)$$

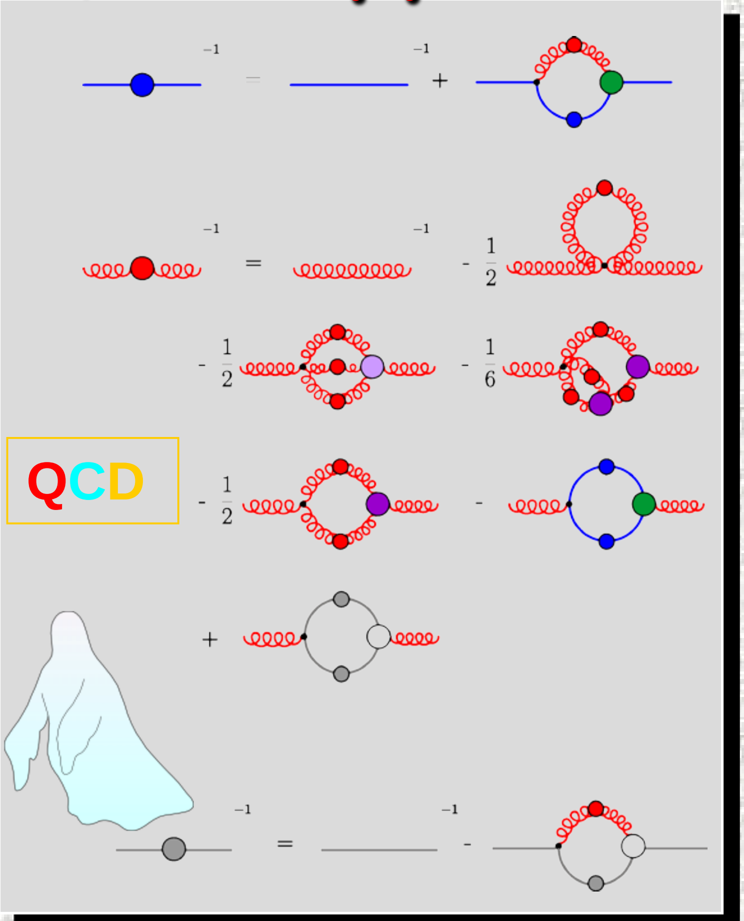

C. D. Roberts, et al, PPNP 33 (1994), 477; 45-S1, 1 (2000); EPJ-ST 140(2007), 53;
R. Alkofer, et. al, Phys. Rep. 353, 281 (2001); LYX, Roberts, et al., CTP 58 (2012), 79; ·

♠ Algorithms of Solving the DSEs of QCD

- **Solving the coupled** quark, ghost and gluon (parts of the diagrams) **equations**, e.g.,

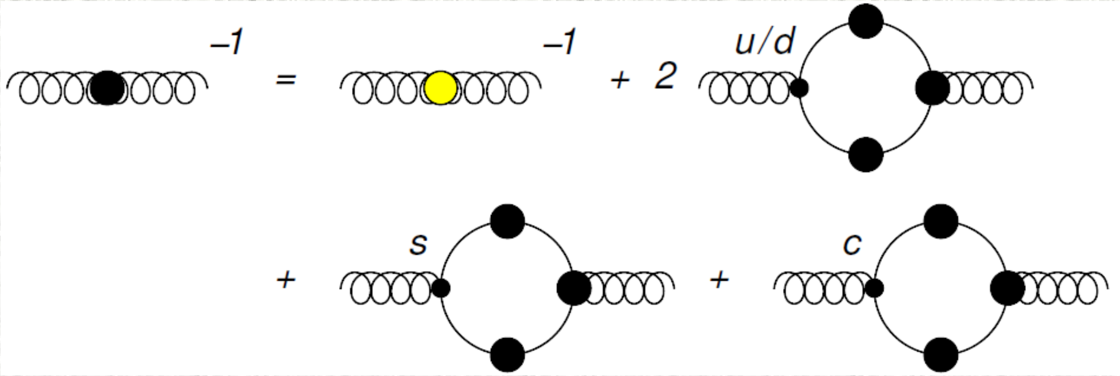

- **Solving the truncated quark equation** with the symmetries being preserved.

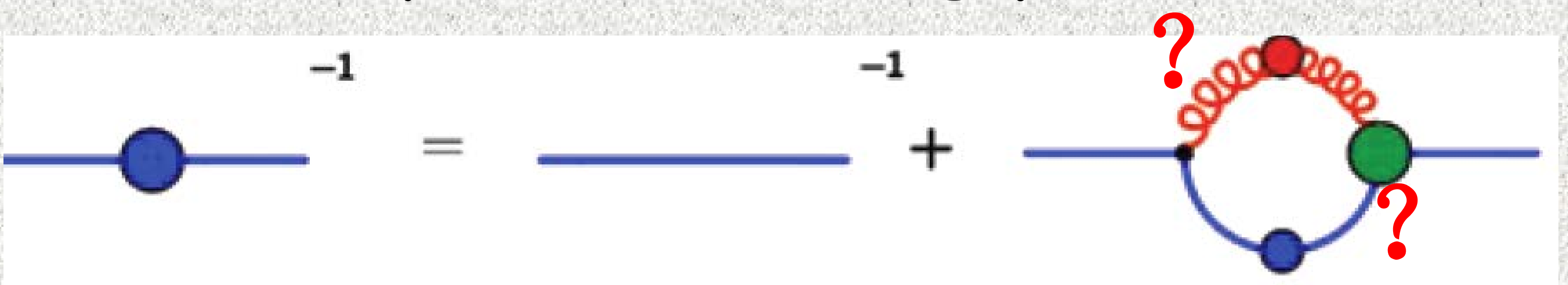

✦ Expression of the quark gap equation

- Truncation: Preserving Symm. ➔ Quark Eq.

$$S^{-1}(p) = Z_2(-i\not{p} + Z_m m) + Z_1 g^2 \int \frac{d^4q}{(2\pi)^4} [t^a \gamma_\mu S(q) \Gamma^b_\nu(p,q) D^{ab}_{\mu\nu}(p-q)]$$

- Decomposition of the Lorentz Structure
  - Quark Eq. in Vacuum :

$$S^{-1}(p) = i\not{p} A(p^2, \Lambda^2) + B(p^2, \Lambda^2)$$

$$\rightarrow \begin{cases} A(x) = 1 + \dfrac{1}{6\pi^3} \displaystyle\int dy \frac{yA(y)}{yA^2(y) + B^2(y)} \Theta_A(x,y) \\ B(y) = \dfrac{1}{2\pi^3} \displaystyle\int dy \frac{yB(y)}{yA^2(y) + B^2(y)} \Theta_B(x,y) \end{cases}$$

• Quark Eq. in Medium

Matsubara Formalism

Temperature T : ➔ Matsubara Frequency

$$\omega_n = (2n+1)\pi T$$

Density ρ : ➔ Chemical Potential μ

$$S^{-1}(p) \Longrightarrow S^{-1}(p, \omega_n, \mu)$$

Decomposition of the Lorentz Structure

$$S^{-1}(p) = i\gamma \cdot p A(p^2) + B(p^2)\,, \quad \Longrightarrow$$

$$S^{-1}(p, \omega_n, \mu) = iA(p, \omega_n, \mu)\vec{\gamma} \cdot \vec{p} + iC(p, \mu)\gamma_4(\omega_n + i\mu) + B(\tilde{p}) + \cdots$$

✦ Models of the eff. gluon propagator

$$g^2 D_{\rho\sigma}(k) = 4\pi \frac{\mathcal{G}(k^2)}{k^2} \left(\delta_{\rho\sigma} - \frac{k_\rho k_\sigma}{k^2}\right)$$

- **Commonly Used: Maris-Tandy Model (PRC 56, 3369)**

$$\frac{\mathcal{G}(t)}{t} = \frac{4\pi^2}{\omega^6} D\, t e^{-t/\omega^2} + \frac{8\pi^2 \gamma_m}{\ln\left[\tau + \left(1 + t/\Lambda_{\rm QCD}^2\right)^2\right]} \frac{1 - \exp(-t/[4m_{\mathcal{F}}^2])}{t} \quad (3)$$

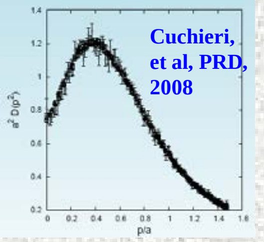

- **Recently Proposed: Infrared Constant Model**

(Qin, Chang, Liu, Roberts, Wilson, Phys. Rev. C 84, 042202(R), (2011).)

Taking $t/\omega^2 = k^2/\omega^2 = 1$ in the coefficient of the above expression

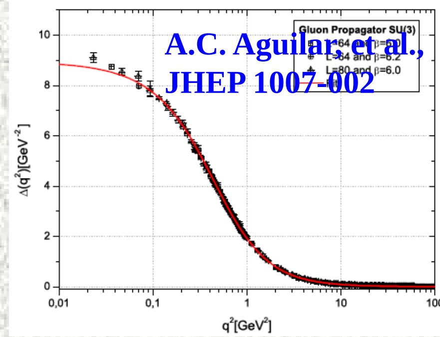

- **Derivation and analysis in PRD 87, 085039 (2013) show that the one in 4-D should be infrared constant.**

✦ Models of quark-gluon interaction vertex

$$\Gamma_\mu^a(q,p) = t^a \Gamma_\mu(q,p)$$

- **Bare Ansatz**

$$\Gamma_\mu(q,p) = \gamma_\mu$$ (Rainbow Approx.)

- **Ball-Chiu (BC) Ansatz**

$$\Gamma_\mu^{BC}(p,q) = \frac{A(p^2)+A(q^2)}{2}\gamma_\mu + \frac{(p+q)_\mu}{p^2-q^2}\{[A(p^2)-A(q^2)]\frac{(\gamma\cdot p+\gamma\cdot q)}{2} - i[B(p^2)-B(q^2)]\}$$

Satisfying W-T Identity, L-C. restricted

- **Curtis-Pennington (CP) Ansatz**

$$\Gamma_\mu^{CP}(p,q) = \Gamma_\mu^{BC}(p,q) + \frac{1}{2}(A(p^2)-A(q^2))\frac{\gamma_\mu(p^2-q^2)-(k+p)_\mu\gamma\cdot(p+q)}{d(p,q)},$$

$$d(p,q) = \frac{(p^2-q^2)^2+[M^2(p^2)+M^2(q^2)]^2}{p^2+q^2}$$

Satisfying Prod. Ren.

- **CLR** (BC+ACM, Chang, etc, PRL 106,072001('11), Qin, etc, PLB 722,384('13))

$$\Gamma_\mu^{\rm acm}(p_f,p_i) = \Gamma_\mu^{{\rm acm}_4}(p_f,p_i) + \Gamma_\mu^{{\rm acm}_5}(p_f,p_i),$$

(2) DSE meets the requirements for an approach to describe the QCD PTs

♠ Dynamical chiral symmetry breaking

$$\boxed{\mathcal{M}(p) \simeq m_0 \, [\ln p/\Lambda_{QCD}]^d + C \frac{-\langle \bar{q}q \rangle}{p^2 \, [\ln p/\Lambda_{QCD}]^d}}$$

$\langle \bar{q} q \rangle \neq 0$ ➡ **DCSB**

In DSE approach

$$M(p^2) = \frac{B(p^2)}{A(p^2)}$$

Numerical results in chiral limit

➔ **Increasing the interaction strength induces the dynamical mass generation**

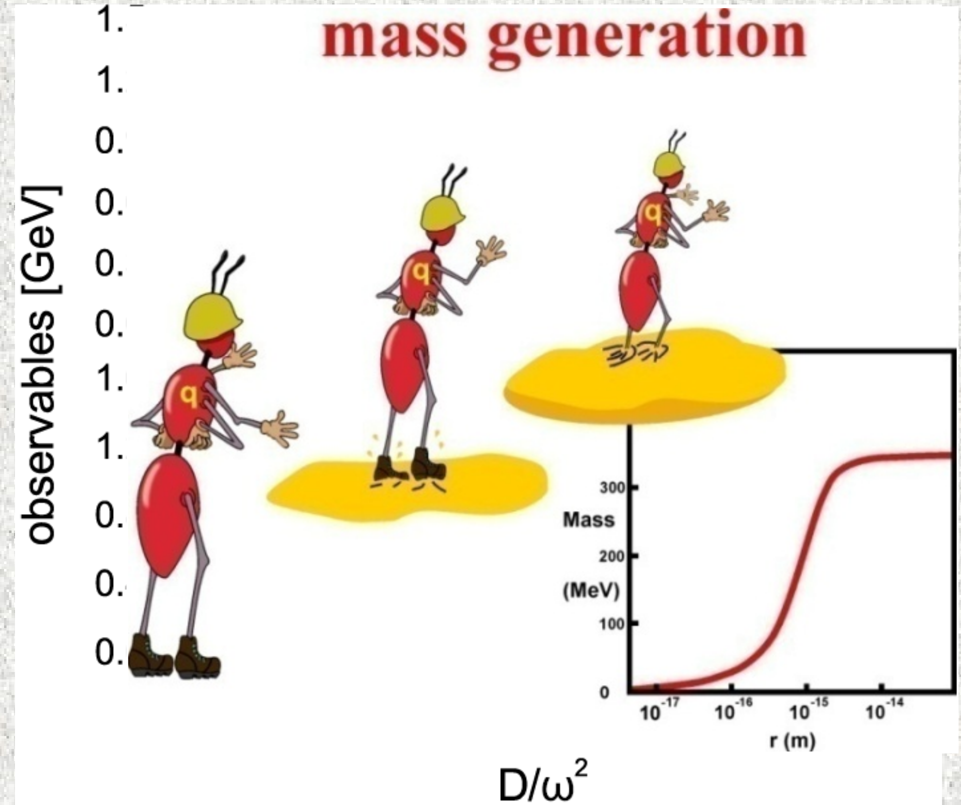

K.L. Wang, YXL, et al., PRD 86,114001('12);

✦ Dynamical Chiral Symmetry Breaking (DCSB) still exists beyond chiral limit

L. Chang, Y. X. Liu, C. D. Roberts, et al, arXiv: nucl-th/0605058;
R. Williams, C.S. Fischer, M.R. Pennington, arXiv: hep-ph/0612061;
K. L. wang, Y. X. Liu, & C. D. Roberts, Phys. Rev. D 86, 114001 (2012).

Solutions of the DSE with MT model and QC model for the effective gluon propagator and bare model and 1BC model for the quark-gluon interaction vertex :

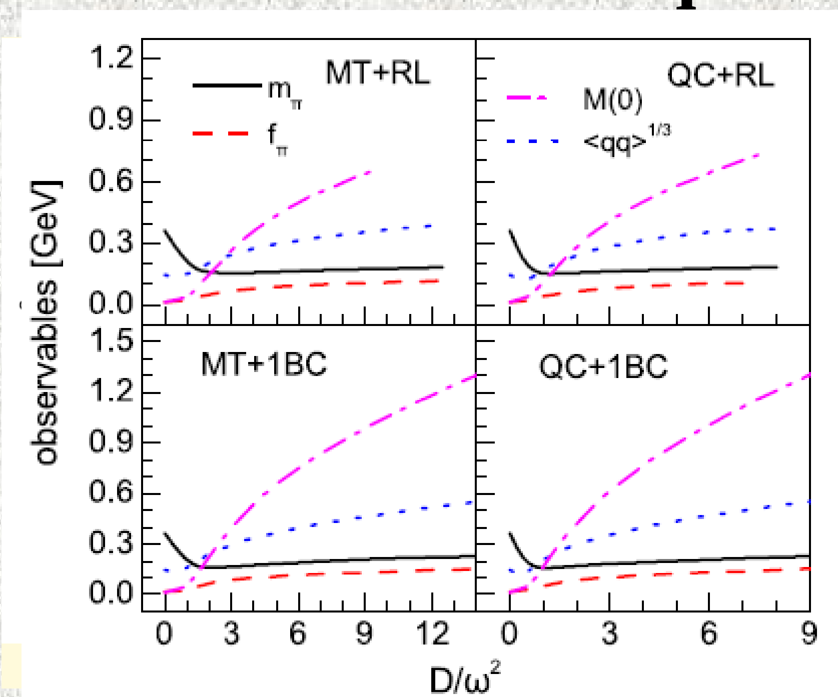

With ω = 0.4 GeV

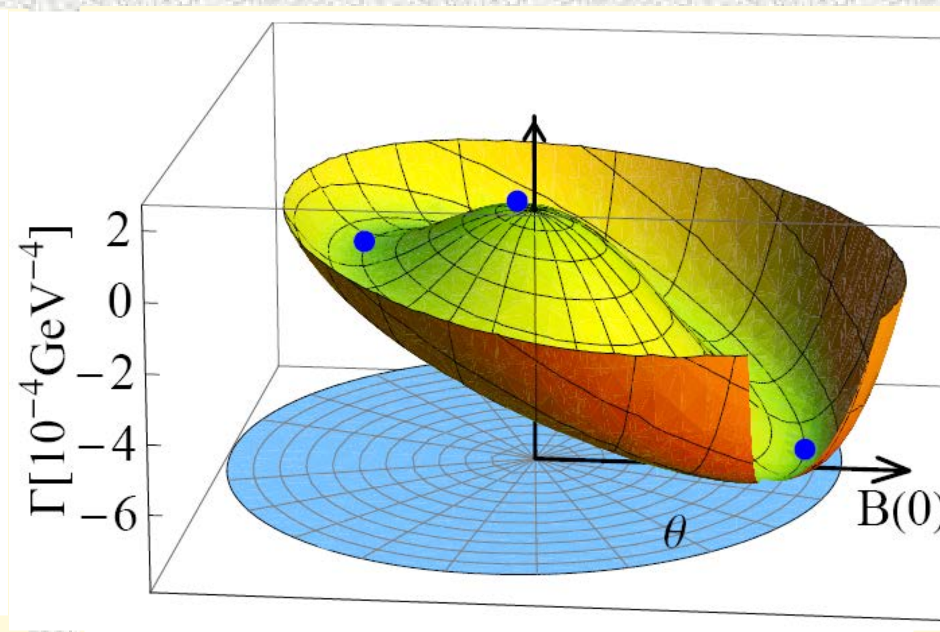

with $D = 16$ GeV^2, $\omega = 0.4$ GeV

♠ Analyzing the spectral density function indicate that the quarks are confined at low temperature and low density

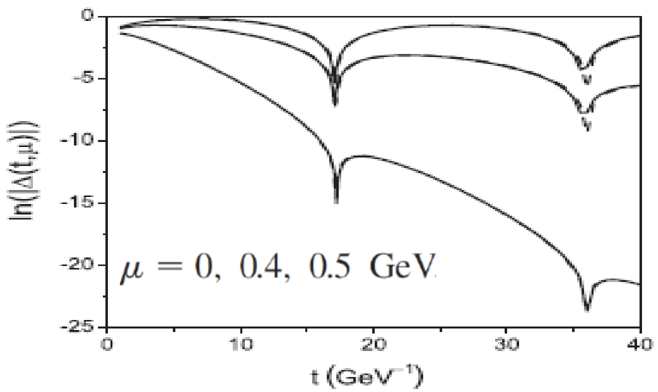

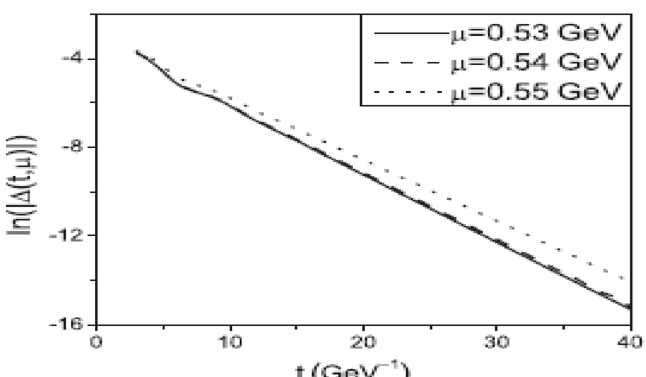

$$\Delta(\tau,\mu) = \int \frac{d^4p}{(2\pi)^4} e^{i\vec{p}\cdot\vec{x}+ip_4\tau}\delta(\vec{p})\sigma_B(p;\mu).$$

H. Chen, YXL, et al., Phys. Rev. D 78, 116015 (2008)

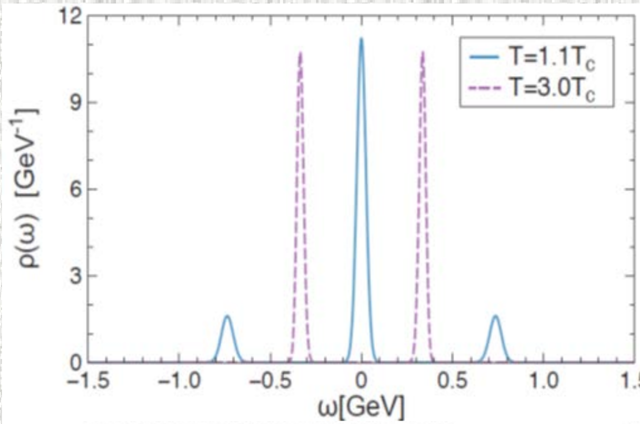

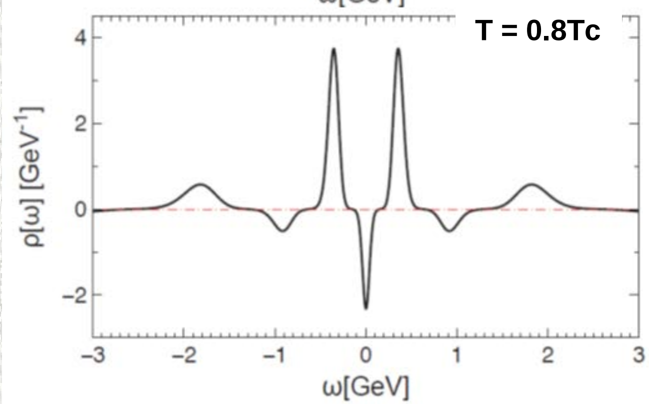

S.X. Qin, D. Rischke, Phys. Rev. D 88, 056007 (2013)

$$S^R(\omega,\vec{p}) = S(i\omega_n,\vec{p})|_{i\omega_n\to\omega+i\epsilon}$$

$$S(i\omega_n,\vec{p}) = \int_{-\infty}^{+\infty}\frac{d\omega'}{2\pi}\frac{\rho(\omega',\vec{p})}{i\omega_n-\omega'}$$

$$\rho(\omega,\vec{p}) = -i\vec{\gamma}\cdot\vec{p}\,\rho_v(\omega,\vec{p}^2) + \gamma_4\omega\,\rho_e(\omega,\vec{p}^2) + \rho_s(\omega,\vec{p}^2)$$

In MEM,

$$P[\rho|M(\alpha)] = \frac{1}{Z_S}e^{\alpha S[\rho,m]},$$

$$S[\rho,m] = \int_{-\infty}^{+\infty} d\omega\left[\rho(\omega) - m(\omega) - \rho(\omega)\ln\frac{\rho(\omega)}{m(\omega)}\right]$$

$$m(\omega) = m_0\theta(\Lambda^2-\omega^2).$$

♠ Hadrons via DSE

♣ Approach 1: Soliton bag model

Pressure difference provides the bag constant.

♣ Approach 2: BSE + DSE

- **Mesons**

BSE with DSE solutions being the input

Quantum field theory bound states: BSE

$$\Gamma_M(p;P) = \int_k^{\Lambda} K(p,k;P)\, S(k_+)\, \Gamma_M(k;P)\, S(k_-)$$

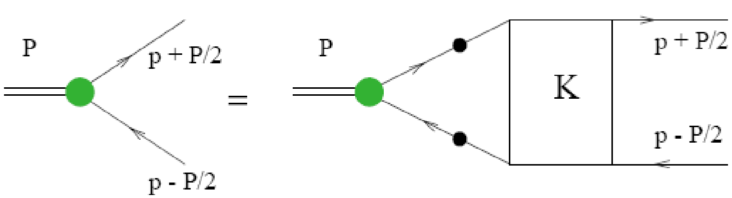

L. Chang, C.D. Roberts, PRL 103, 081601 (2009)。

- **Baryons**

Fadeev Equation or Diquark model (BSE+BSE)

✦ Some properties of mesons in DSE-BSE

Solving the 4-dimenssional covariant B-S equation with the kernel being fixed by the solution of DS equation and flavor symmetry breaking, we obtain

	Expt. (GeV)	Calc. (GeV)	Th/
“ρ^0”	0.7755	0.7704	
$\rho^{\pm}$	0.7755	0.7755	
“ω”	0.7827	0.7806	
$K^{*\pm}$	0.8917	0.8915	
K^{*0}	0.8960	0.8969	
ϕ	1.0195	1.0195	
D^{*0}	2.0067	1.8321	
$D^{*\pm}$	2.0100	1.8387	
$D_s^{*\pm}$	2.1120	1.9871	
J/ψ	3.0969	3.0969	
$B^{*\pm}$		4.8543	
B^{*0}		4.8613	
B_s^{*0}		5.0191	
$B_c^{*\pm}$		6.2047	
Υ	9.4603	9.4603	

	Expt. (GeV)	Calc. (GeV)	Th/Ex-1 (%)
π^0	0.13498	0.13460	-0.3
$\pi^{\pm}$	0.13957	0.13499	-3.3
$K^{\pm}$	0.49368	0.41703	-15.5
K^0	0.49765	0.42662	-14.3
η	0.54751	0.45499	-16.9
η'	0.95778	0.91960	-4.0
D^0	1.8645	1.6195	-13.1
$D^{\pm}$	1.8693	1.6270	-13.0
$D_s^{\pm}$	1.9682	1.7938	-8.9
η_c	2.9804	3.0171	1.2
$B^{\pm}$	5.2790	4.7747	-9.6
B^0	5.2794	4.7819	-9.4
B_s^0	5.3675	4.9430	-7.9
$B_c^{\pm}$	6.286	6.1505	-2.2
η_b	9.300	9.4438	1.5

(L. Chang, Y. X. Liu, C. D. Roberts, et al., Phys. Rev. C 76, 045203 (2007))

✦ Some properties of mesons in DSE-BSE

	Present work	Expt.	RL-Padé	RL-direct
m_π	0.138	0.138	0.138	0.137
m_ρ	0.84 ± 0.03	0.777	0.754	0.758
m_σ	1.13 ± 0.01	$0.4 - 1.2$	0.645	0.645
m_{a_1}	1.28 ± 0.01	1.24 ± 0.04	0.938	0.927
m_{b_1}	1.24 ± 0.10	1.21 ± 0.02	0.904	0.912
$m_{a_1} - m_\rho$	0.44 ± 0.04	0.46 ± 0.04	0.18	0.17
$m_{b_1} - m_\rho$	0.40 ± 0.14	0.43 ± 0.02	0.15	0.15

(L. Chang, & C.D. Roberts, Phys. Rev. C 85, 052201(R) (2012))

(S.X. Qin, L. Chang, Y.X. Liu, C.D. Roberts, et al., Phys. Rev. C 84, 042202(R) (2011))

✦ T-dependence of the screening masses of some hadrons

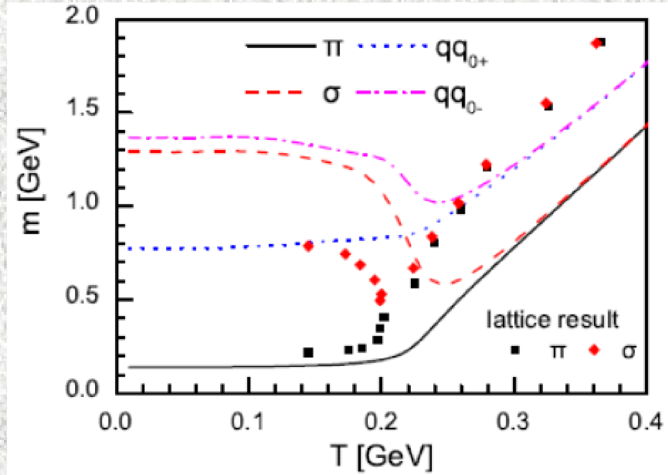

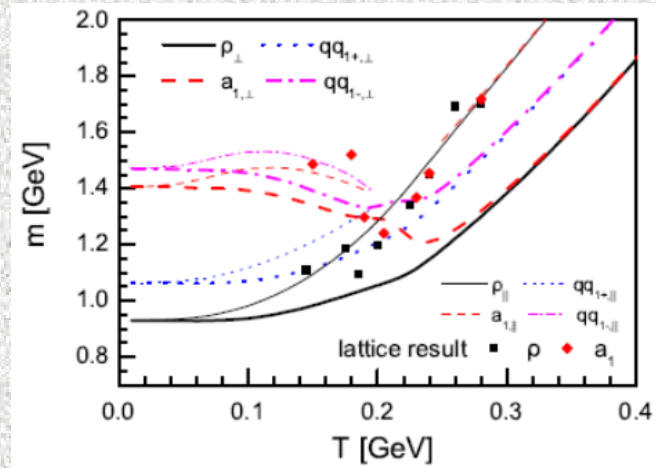

GT Relation

$$M_\sigma^2 = M_\pi^2 + 4M_q^2$$

➔ $M_\sigma \cong M_\pi$ can be a signal of the DCS.

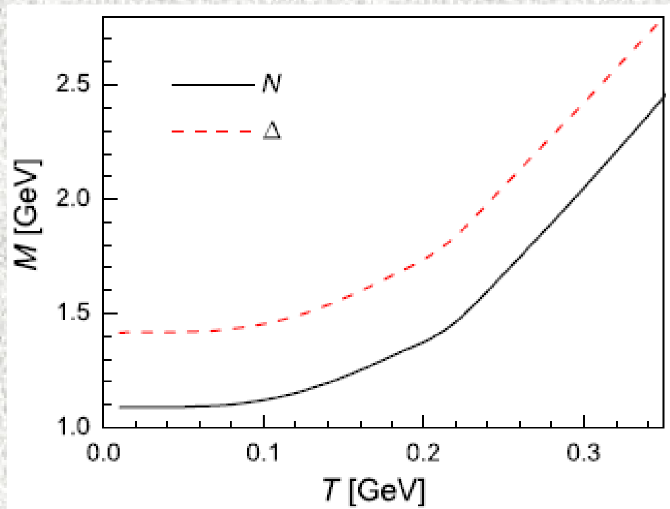

$r_S \propto 1/M_S$, when $r_S < r_{md}$, the color gets deconfined.

Hadron properties provide signals for not only the chiral phase transt. but also the confinement-deconfnmt. phase transition.

Wei-jie Fu, and Yu-xin Liu, Phys. Rev. D 79, 074011 (2009) ;
K.L. Wang, Y.X. Liu, C.D. Roberts, Phys. Rev. D 87, 074038 (2013)

✦ Electromagnetic Property & PDF of hadrons

Pion electromagnetic form factor

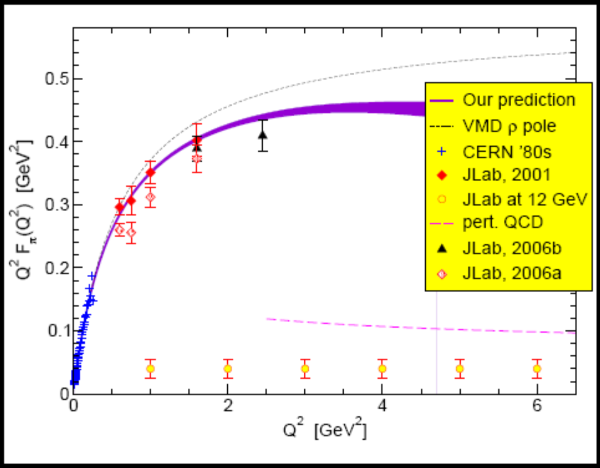

PM and Tandy, PRC62,055204 (2000) [nucl-th/0005015]

P. Maris & PCT, PRC 61, 045202 ('00)

Proton electromagnetic forma factor

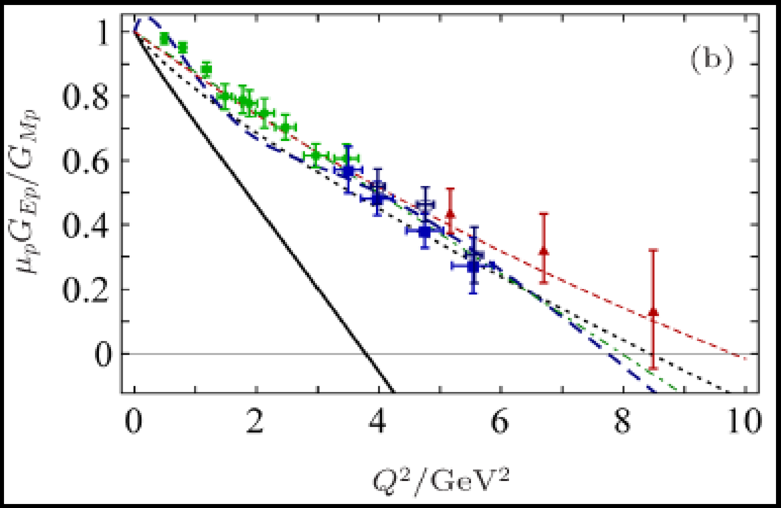

L. Chang et al., AIP CP 1354, 110 ('11)

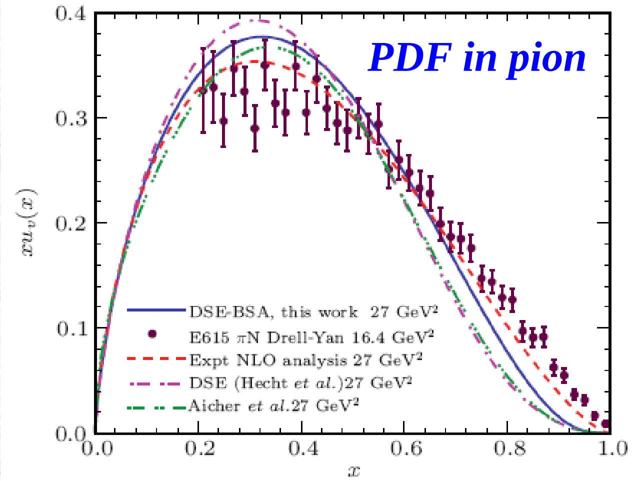

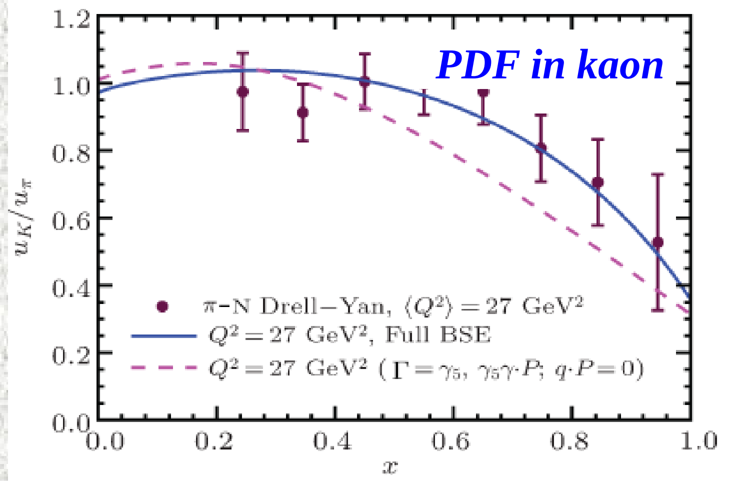

R.J. Holt & C.D. Roberts, RMP 82, 2991(2010); T. Nguyan, CDR, et al., PRC 83, 062201 (R) (2011)

✦ Decay width of $\eta_c \to \gamma^* \gamma$

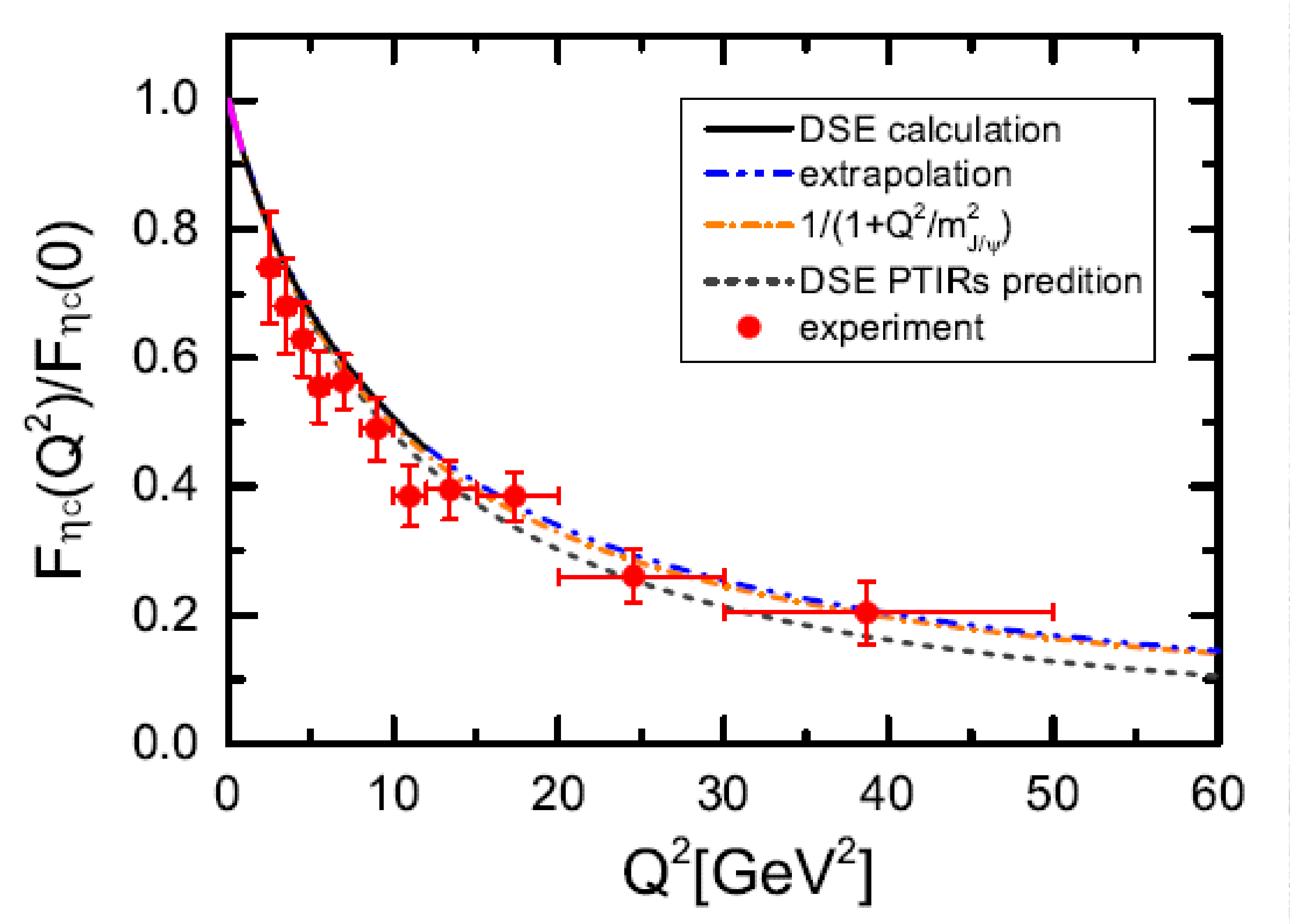

J. Chen, Ming-hui Ding, Lei Chang, and Yu-xin Liu, Phys. Rev. D 95, 016010 (2017)

♠ A theoretical check on the CLR model for the quark-gluon interaction vertex

Physics Letters B 742 (2015) 183–188

Contents lists available at ScienceDirect

Physics Letters B

www.elsevier.com/locate/physletb

Bridging a gap between continuum-QCD and *ab initio* predictions of hadron observables

Daniele Binosi [a], Lei Chang [b], Joannis Papavassiliou [c], Craig D. Roberts [d,*]

$$\mathcal{I}_{\hat{d}}(k^2) := k^2 d(k^2) = \frac{\alpha_s(\zeta^2)\Delta(k^2;\zeta^2)}{[1+G^2(k^2;\zeta^2)]^2}$$

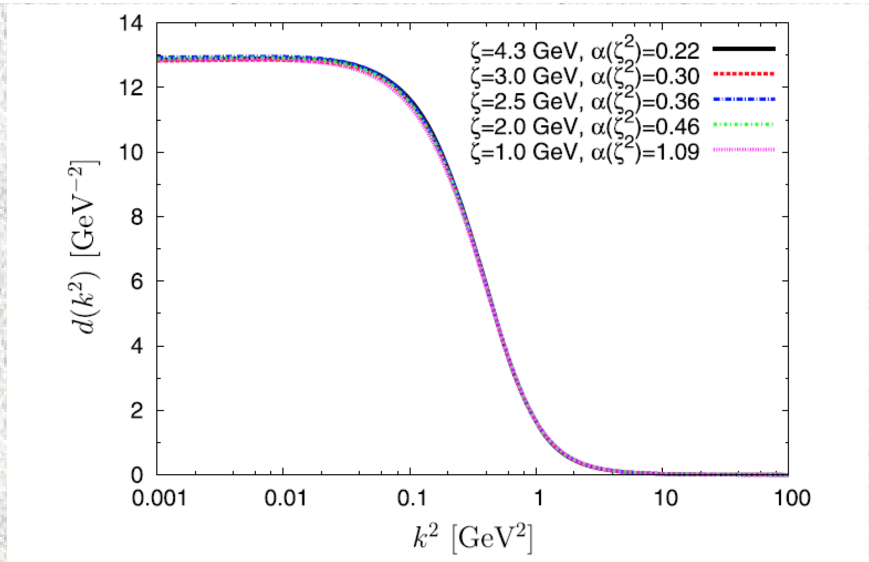

Fig. 1. RGI running interaction strength, $d(k^2)$ in Eq. (19), computed via a combination of DSE- and lattice-QCD results, as explained in Ref. [25]. We display the

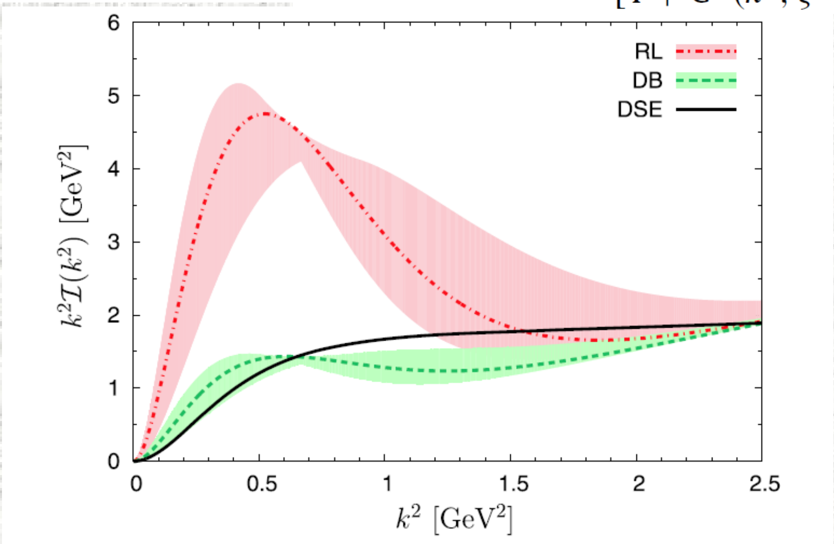

Fig. 2. Comparison between top-down results for the gauge-sector interaction [Eqs. (19), (22), Fig. 1] with those obtained using the bottom-up approach based on hadron physics observables [Eqs. (4)–(8)]. *Solid curve* – top-down result for the

♠ A comment on the DSE approach of QCD

Available online at www.sciencedirect.com

ScienceDirect

ELSEVIER

NUCLEAR PHYSICS A

Nuclear Physics A 796 (2007) 83–100

Phases of dense quarks at large N_c

Larry McLerran [a,b], Robert D. Pisarski [a,*]

[a] Physics Department, Brookhaven National Laboratory, Upton, NY 11973, USA
[b] RIKEN BNL Research Center, Brookhaven National Laboratory, Upton, NY 11973, USA

Received 15 July 2007; received in revised form 14 August 2007; accepted 15 August 2007

Available online 14 September 2007

One way of computing the properties of a quarkyonic phase is to use approximate solutions of Schwinger–Dyson equations [23]. These are, almost uniquely, the one approximation scheme which includes both confinement and chiral symmetry breaking. They do have features reminiscent of large N_c: at low momentum, if chiral symmetry breaking occurs, the gluon propagator for $N_f = 3$ is numerically close to that for $N_f = 0$. At present, solutions at $\mu \neq 0$ assume a Fermi surface dominated by quarks; if quark screening is not too large at moderate μ, these models should exhibit a quarkyonic phase.

C. D. Roberts, et al, PPNP 33 (1994), 477; 45-S1, 1 (2000); EPJ-ST 140(2007), 53;
R. Alkofer, et. al, Phys. Rep. 353, 281 (2001); LYX, et al., CTP 58, 79 (2012); …… .

III. Criteria of the Phase Transitions

♠ Conventional Criterion

Order Parameter: chiral cond. $\langle\bar{q}q\rangle$!

$$\mathcal{M}(p) \simeq m_0 \left[\ln p/\Lambda_{QCD}\right]^d + C \frac{-\langle\bar{q}q\rangle}{p^2\left[\ln p/\Lambda_{QCD}\right]^d}$$

Procedure: Analyzing the TD Potential

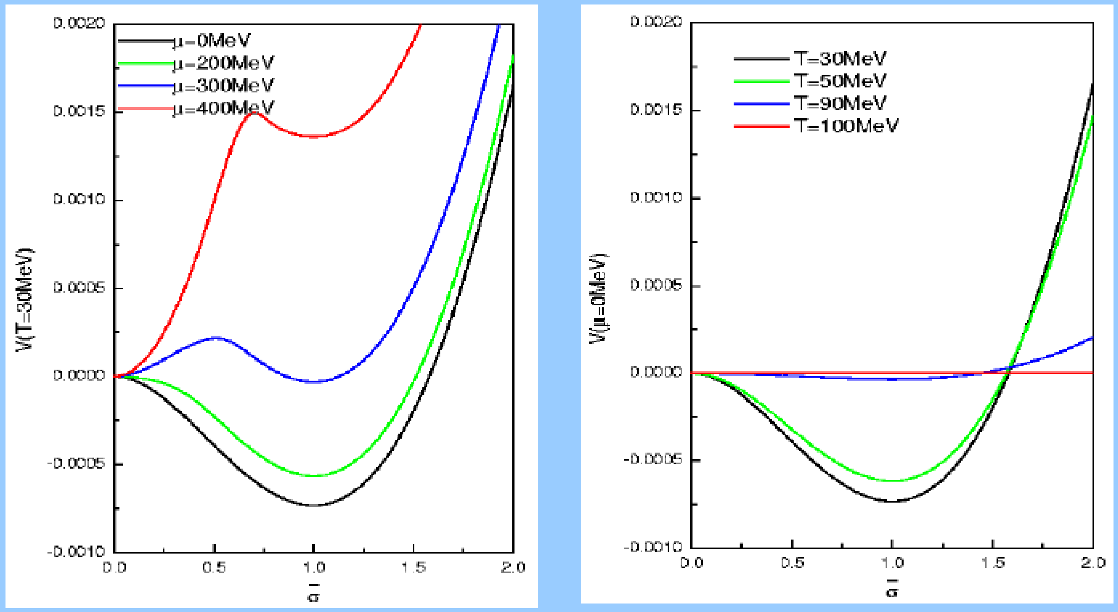

$$\text{Criteria of } PT: \frac{\partial^2\Omega}{\partial T^2}, \frac{\partial^2\Omega}{\partial \mu^2}, \text{ etc, change sign .}$$

• Critical phenomenon can be a criterion for CEP

$$\chi = \frac{\partial \rho}{\partial \mu} = \frac{\partial^2 P}{\partial \mu^2}$$

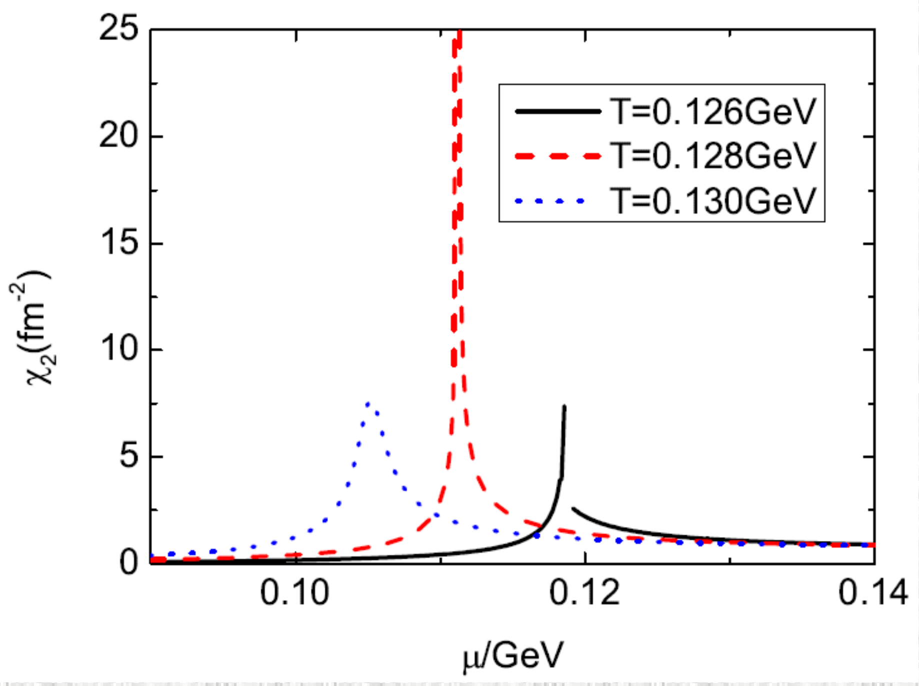

$$\varepsilon = T^2 \frac{\partial P/T}{\partial T} \quad c_V = \frac{\partial \varepsilon}{\partial T}$$

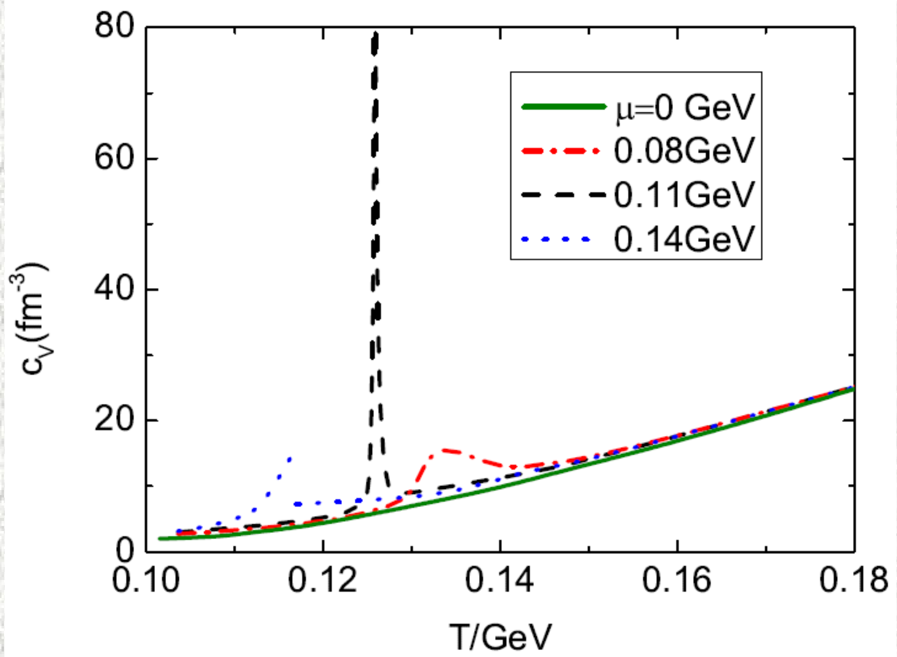

Gao, Chen, Liu, Qin, Roberts, Schmidt, Phys. Rev. D 93, 094019 (2016).

• Locating the CEP with the Critical Behavior

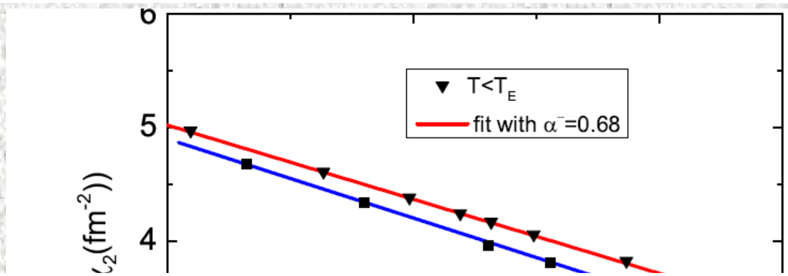

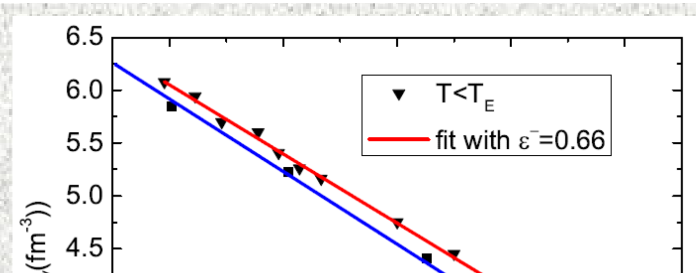

Quantity	$T-T_E\to 0^+$	$T-T_E\to 0^-$	$\mu-\mu_E\to 0^+$	$\mu-\mu_E\to 0^-$
c_V	0.69 ± 0.02	0.66 ± 0.01	0.69 ± 0.01	0.65 ± 0.01
χ_q	0.69 ± 0.01	0.68 ± 0.01	0.68 ± 0.01	0.65 ± 0.02

$$(\mu_E^\chi, T_E^\chi) = (110.9, 127.5)\ \mathrm{MeV}$$

Question: In complete nonperturbation, one can not have the thermodynamic potential.

The conventional criterion fails.

One needs then new criterion!

Gao, Chen, Liu, Qin, Roberts, Schmidt, Phys. Rev. D 93, 094019 (2016).

♠ New Criterion: Chiral Susceptibility

- **Def.: Resp. the OP to control variables**

$$\frac{\partial M}{\partial T}, \quad \frac{\partial M}{\partial \mu}; \qquad \frac{\partial \langle \bar{q} q \rangle}{\partial T}, \quad \frac{\partial \langle \bar{q} q \rangle}{\partial \mu}; \qquad \frac{\partial B}{\partial T}, \quad \frac{\partial B}{\partial \mu}; \qquad \frac{\partial B}{\partial m_0};$$

- **Simple Demonst. Equiv. of NewC to ConvC**

（刘玉鑫，《热学》，北京大学出版社，2016年第1版）

TD Potential: $\Omega(T,\eta) = \Omega_0(T) + \frac{1}{2}\alpha\eta^2 + \frac{1}{4}\beta(\eta^2)^2 + \frac{1}{6}\gamma(\eta^2)^3 + \cdots$

Stability Condition: $\frac{\partial \Omega}{\partial \eta} = \alpha\eta + \beta\eta^3 + \gamma\eta^5 = 0$

$$\frac{\partial^2 \Omega}{\partial \eta^2} = \alpha + 3\beta\eta^2 + 5\gamma\eta^4 > 0, \ St.; \ < 0, \ Unst..$$

Derivative of ext. cond. against control. var.:

$$[\alpha + 3\beta\eta^2 + 5\gamma\eta^4]\left(\frac{\partial \eta}{\partial \varsigma}\right)_{\varsigma=\zeta_c} + \eta\left(\frac{\partial \alpha}{\partial \varsigma}\right)_{\varsigma=\zeta_c} + \eta^3\left(\frac{\partial \beta}{\partial \varsigma}\right)_{\varsigma=\zeta_c} + \eta^5\left(\frac{\partial \gamma}{\partial \varsigma}\right)_{\varsigma=\zeta_c} = 0$$

we have: $\chi = \left(\frac{\partial \eta}{\partial \varsigma}\right)_{\varsigma=\zeta_c} = -\frac{\eta\left(\frac{\partial \alpha}{\partial \varsigma}\right)_{\varsigma=\zeta_c} + \eta^3\left(\frac{\partial \beta}{\partial \varsigma}\right)_{\varsigma=\zeta_c} + \eta^5\left(\frac{\partial \gamma}{\partial \varsigma}\right)_{\varsigma=\zeta_c}}{\left(\frac{\partial^2 \Omega}{\partial \eta^2}\right)_{\frac{\partial \Omega}{\partial \eta}=0}}$

At field theory level, see Fei Gao, Y.X. Liu, Phys. Rev. D 94, 076009 (2016) .

♣Demonstration of the New Criterion

In chiral limit（$m_0 = 0$）

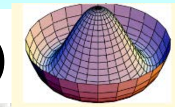

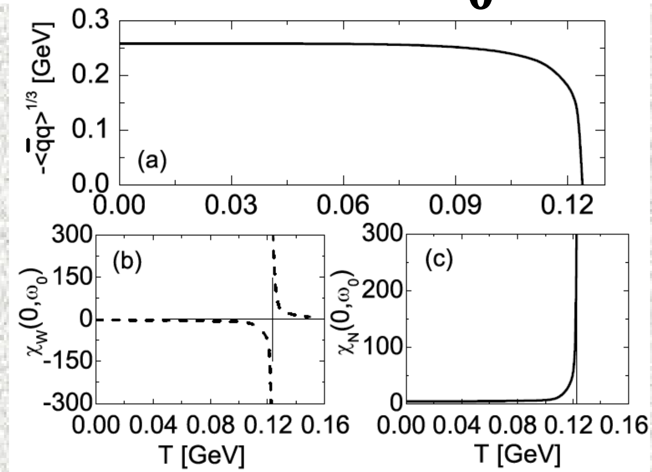

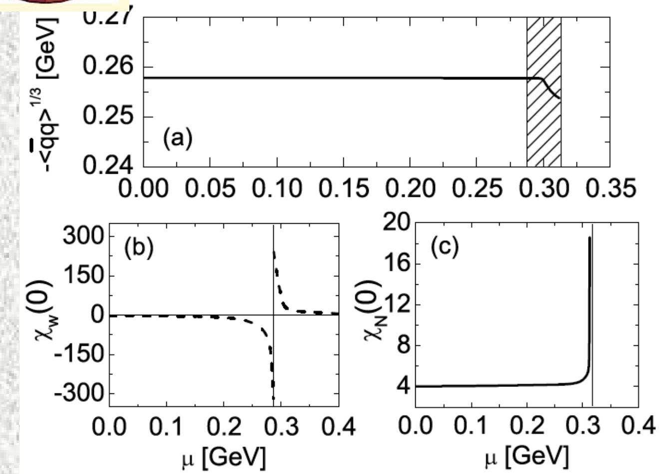

S.X. Qin, L. Chang, H. Chen, YXL, et al., Phys. Rev. Lett. 106, 172301 (2011).

Beyond chiral limit（$m_0 \neq 0$）

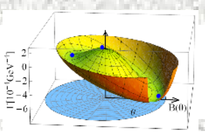

$$\langle\bar{q}q\rangle = \langle\bar{q}q\rangle_{m_0} - m_0\frac{\partial\langle\bar{q}q\rangle_{m_0}}{\partial m_0}$$

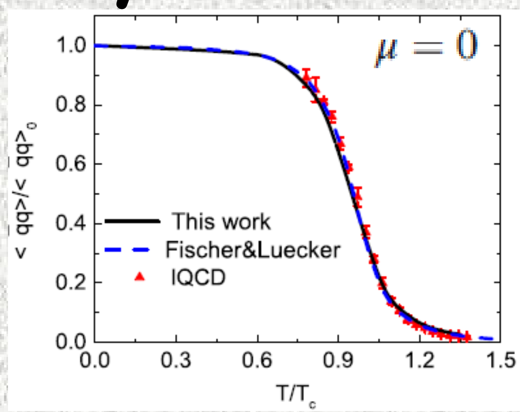

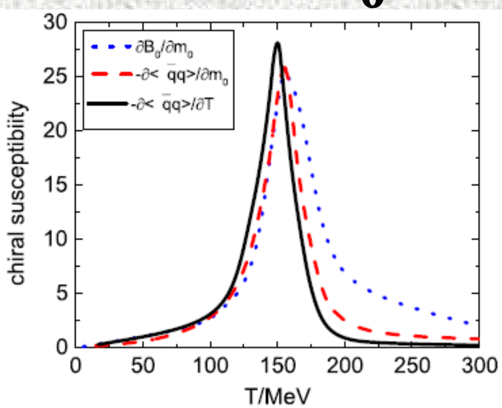

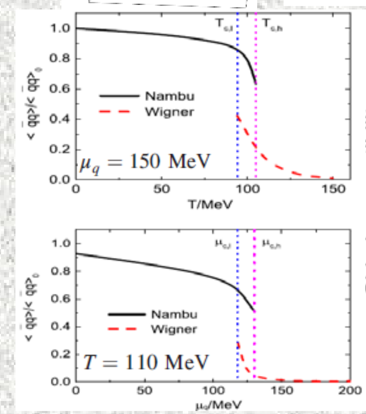

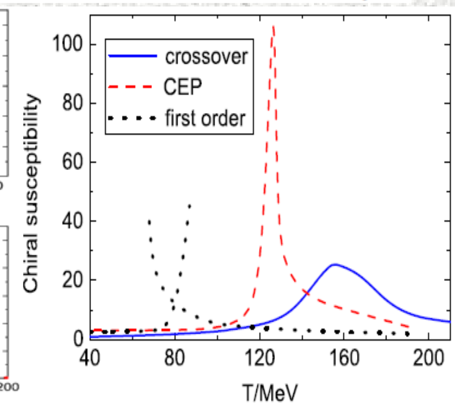

Fei Gao, Y.X. Liu, Phys. Rev. D 94, 076009 (2016) .

♣ Characteristic of the New Criterion

As 2nd order PT (Crossover) occurs,
the χs of the two (DCS, DCSB) phases diverge (take maximum) at same states.

As 1st order PT takes place,
χs of the two phases diverge at dif. states.

➔ the χ criterion can not only give the phase boundary, but also determine the position the CEP.

For multi-flavor system,

one should analyze the maximal eigenvalue of the susceptibility matrix (L.J. Jiang, YXL, et al., PRD 88, 016008),
or the mixed susceptibility (F. Gao, YXL, PRD 94, 076009).

♠ A easily calculated criterion of the conf.

General expression of the Schwinger function

$$D_\pm(\tau, |\vec{p}|=0) = T\sum_n e^{-i\omega_n\tau} S_\pm(i\omega_n+\mu, |\vec{p}|=0)$$
$$= \int_{-\infty}^{+\infty} \frac{d\omega}{2\pi} \rho_\pm(\omega, |\vec{p}|=0) \frac{e^{-(\omega+\mu)\tau}}{1+e^{-(\omega+\mu)/T}},$$

It can be positive, even if the $\rho_\pm$ is negative.

Extending $D_\pm$ to

$$D_\pm^{2n}(\tau, |\vec{p}|)$$
$$= \int_{-\infty}^{+\infty} \frac{d\omega}{2\pi} (\omega+\mu)^{2n} \rho_\pm(\omega, |\vec{p}|) \frac{e^{-(\omega+\mu)\tau}}{1+e^{-(\omega+\mu)/T}},$$

the consistence can be guaranteed.

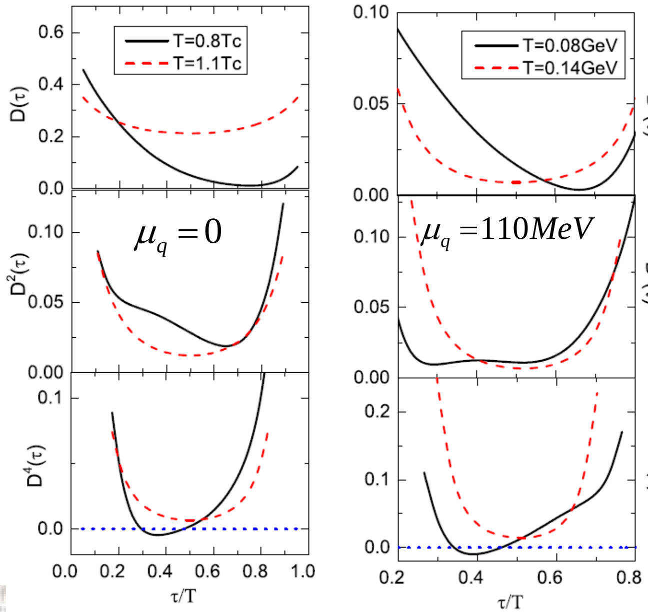

Fei Gao, Y.X. Liu, Phys. Rev. D 94, 076009 (2016) .

♠ Viscosity to Entropy Density Ratio

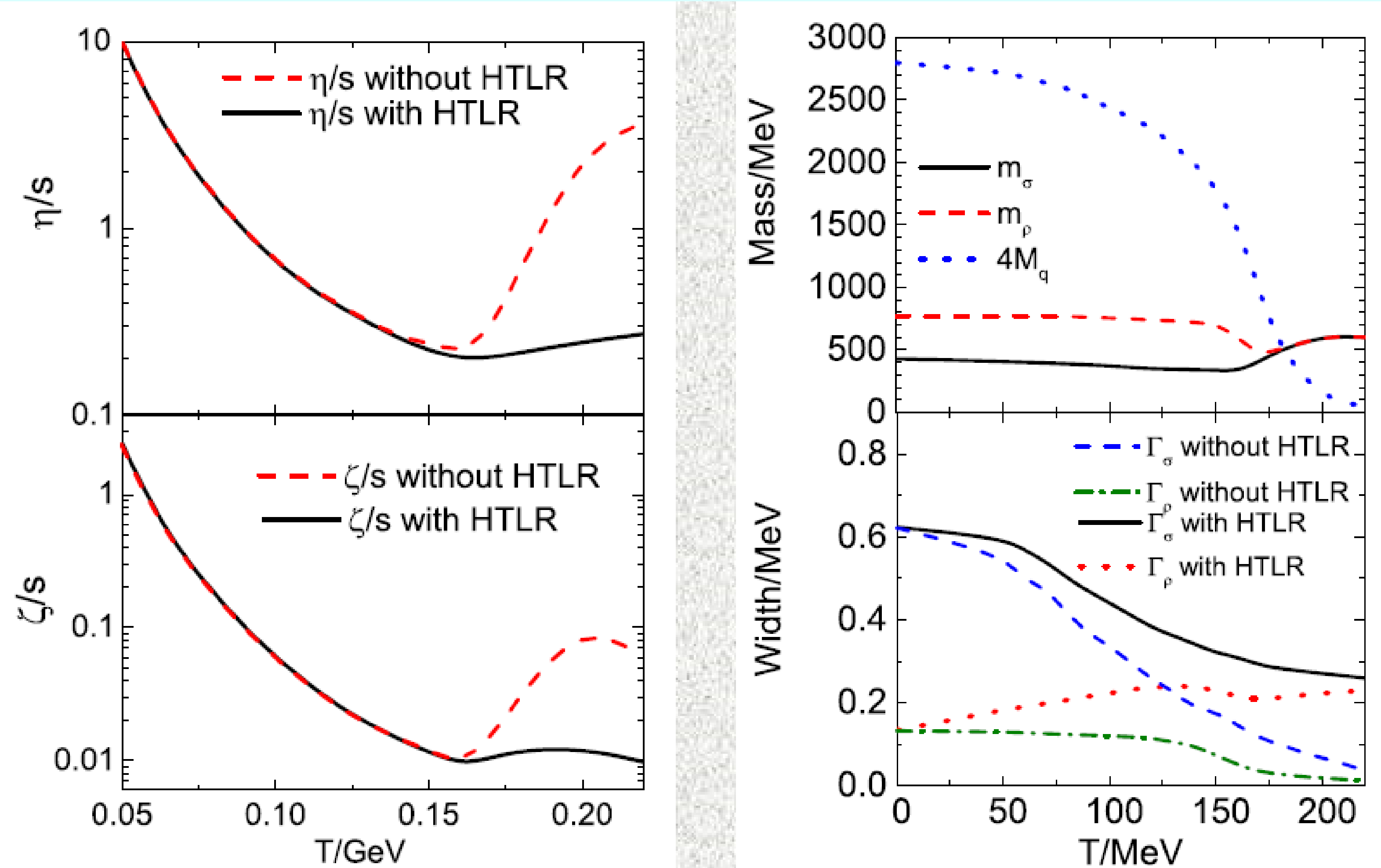

Fei Gao, Y.X. Liu, Phys. Rev. D 97, 056011 (2018) .

- viscosity to entropy density ratios can be the criterion of both the PTs

IV. The QCD Phase Diagrams and the position of the CEP

- **In chiral limit**

With bare vertex
(ETP is available, the PB is shown as the dot-dashed line)

With Ball-Chiu vertex
(ETP is not available, but the coexistence region is obtained)

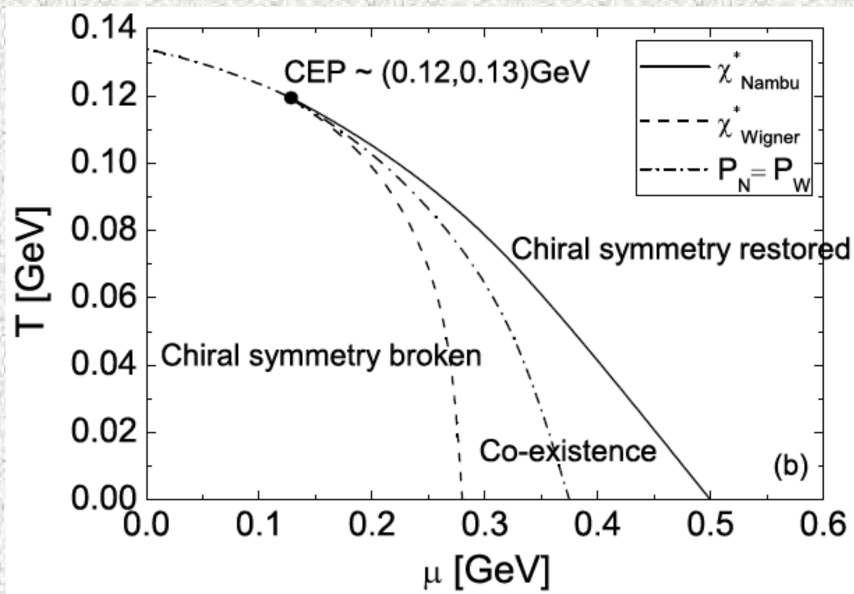

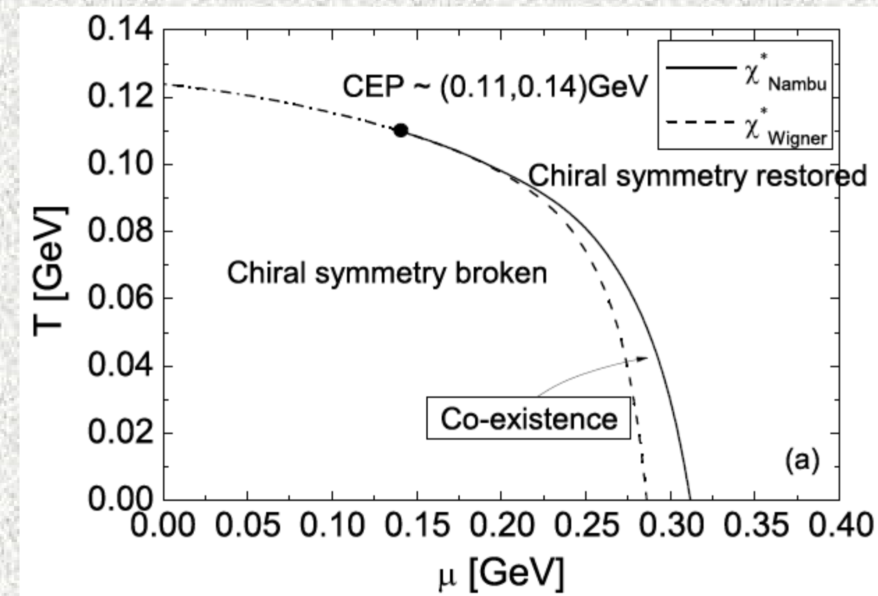

S.X. Qin, L. Chang, H. Chen, YXL, et al., Phys. Rev. Lett. 106, 172301 (2011).

♣ QCD Phase Diagrams and the position of the CEP

- **Beyond chiral limit**

With bare vertex

(ETP is available, the PB is shown as the dot-dashed line)

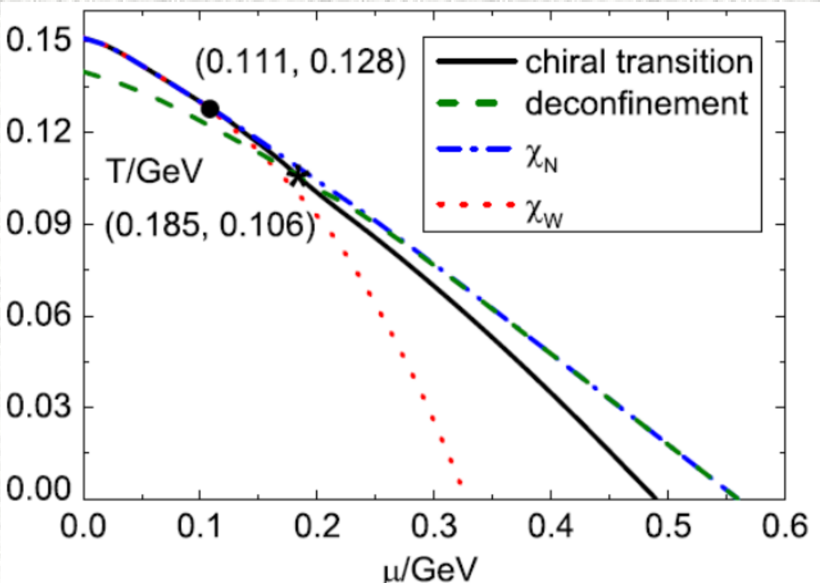

F. Gao, J. Chen, Y.X. Liu, et al., Phys. Rev. D 93, 094019 (2016).

With CLR vertex

(ETP is not available, but the coexistence region is obtained)

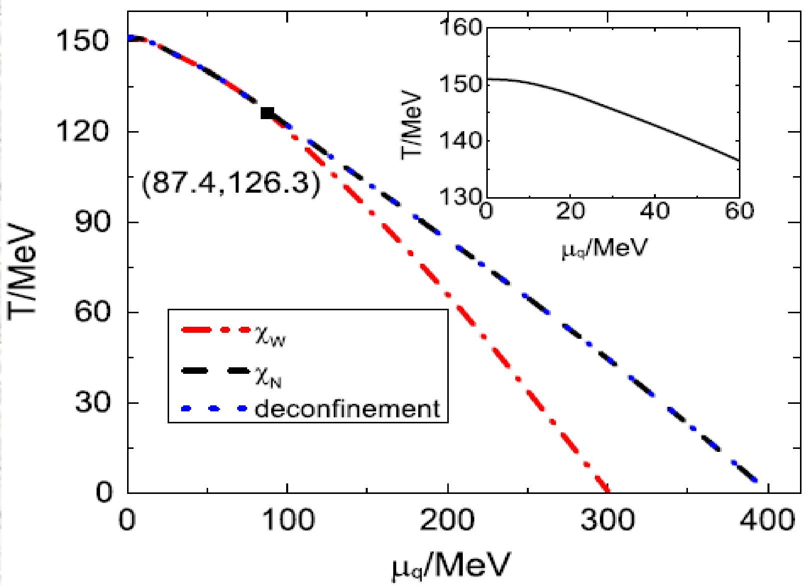

F. Gao, Y.X. Liu, Phys. Rev. D 94, 076009 (2016).

♠ A Lab Observable: BN Fluctuations

Quark number D. Avd: $-\dfrac{\delta\Omega[\mu_X;T]}{\delta\mu_X} = \int d^4x\langle\hat{n}(x)\rangle = \overline{N_X}$

The 2nd and higher order fluctuations

$$\chi_2^X = \frac{1}{VT^3}\langle\delta N_X{}^2\rangle, \qquad \chi_4^X = \frac{1}{VT^3}(\langle\delta N_X{}^4\rangle - 3\langle\delta N_X{}^2\rangle^2),$$

$$\chi_6^X = \frac{1}{VT^3}(\langle\delta N_X{}^6\rangle - 15\langle\delta N_X{}^4\rangle\langle\delta N_X{}^2\rangle - 10\langle\delta N_X{}^3\rangle^2 + 30\langle\delta N_X{}^2\rangle^3).$$

where $\delta N_X = N_X - \langle N_X\rangle$.

$$N_q(\mu,T)\cdot T^3 = \frac{\partial P}{\partial\mu_q} = \frac{1}{\beta V}\int d^4x\langle\bar{q}(x)\gamma_4 q(x)\rangle = 2N_c N_f Z_2\int_{-\infty}^{\infty}\frac{d^3\vec{p}}{(2\pi)^3}f_1(\vec{p};\mu,T)\,,$$

$$f_1(\vec{p};\mu,T) = \frac{T}{2}\sum_{m=-\infty}^{\infty}\mathrm{tr}_{\mathrm{D}}(-\gamma_4 S(\tilde{\omega}_m,\vec{p}))\,,$$

For 2-flavor system: $N_B = \frac{1}{3}N_q,\ \ \mu_B = 3\mu_q$.

Skewness & kurtosis: $\frac{\chi_3}{\chi_2} = S\sigma,\ \ \frac{\chi_4}{\chi_2} = \kappa\sigma^2$.

✦ Quark Number Density Fluctuations and their ratios vs T & μ in the DSE

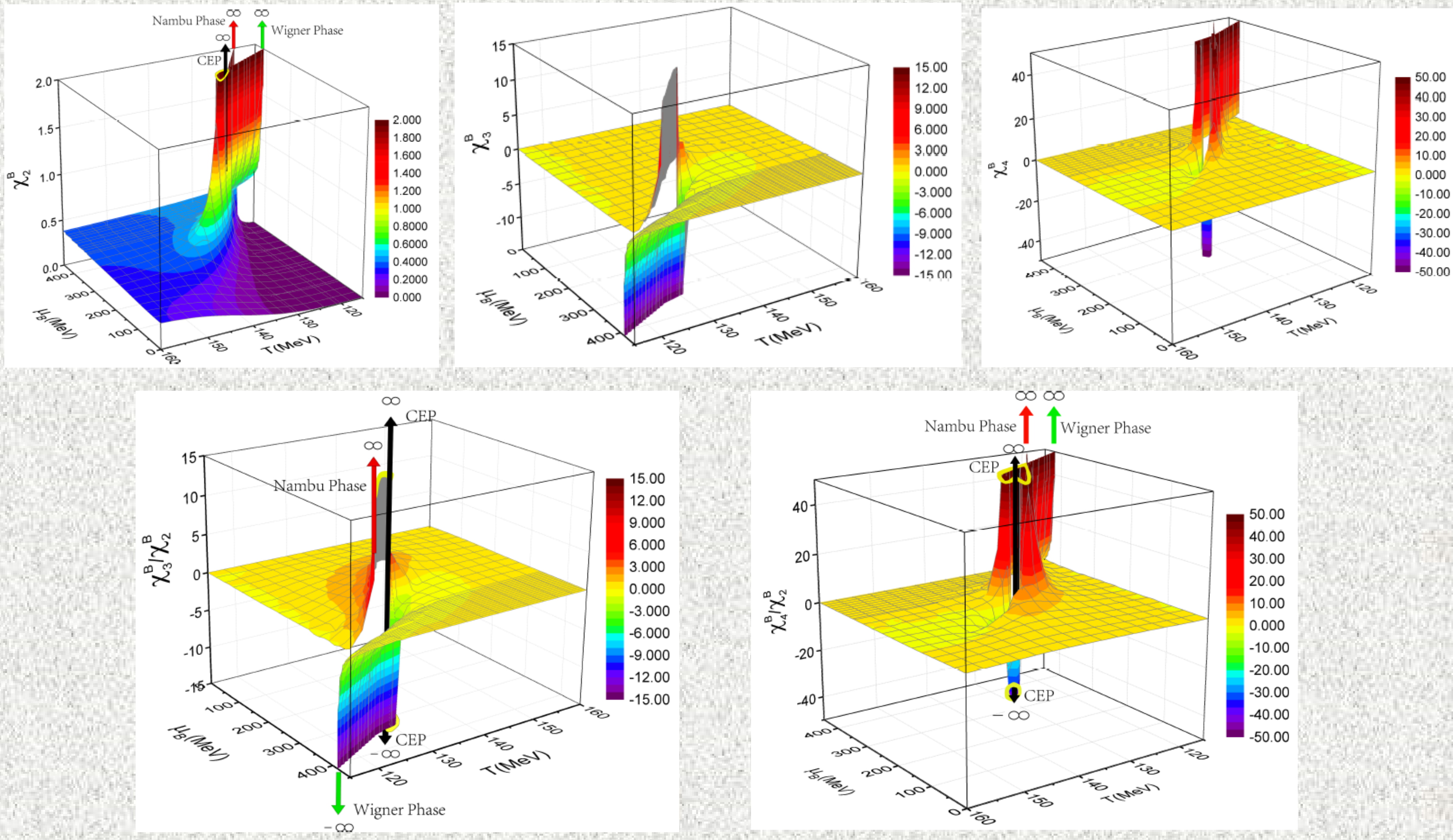

Jing Chen, Fei Gao, Yu-xin Liu, to be published

✦ Quark Number Density Fluctuations vs T in the DSE

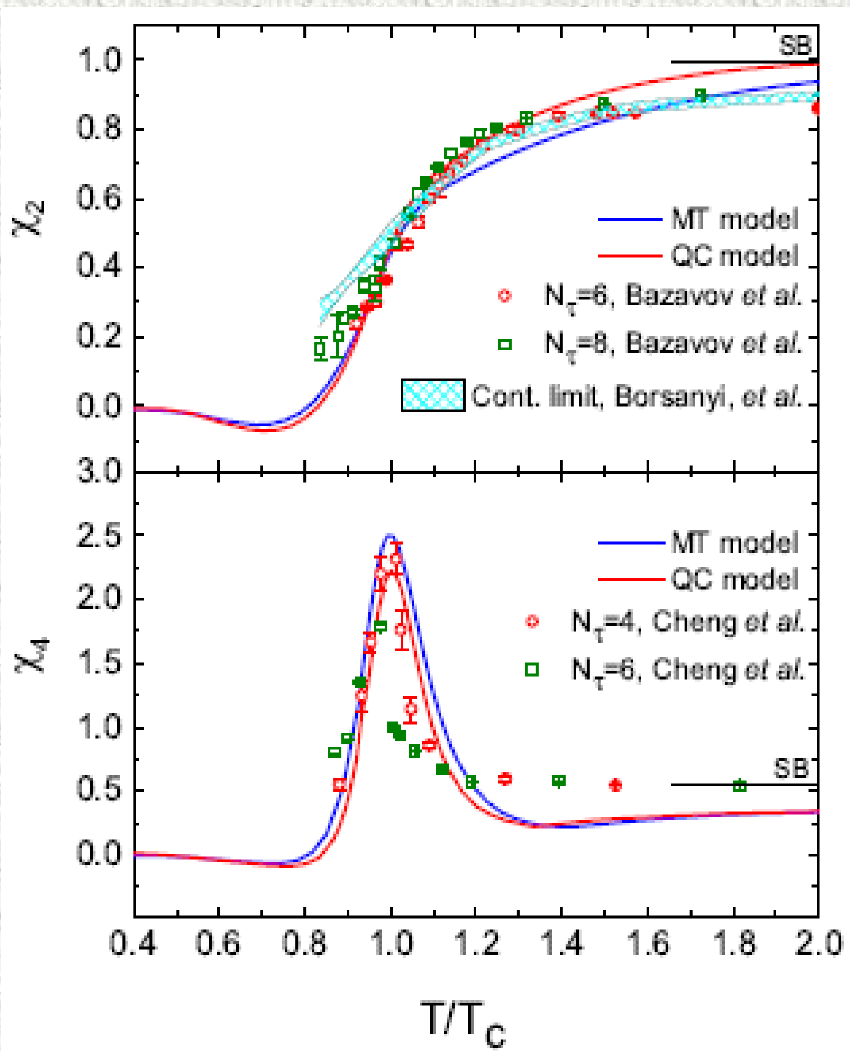

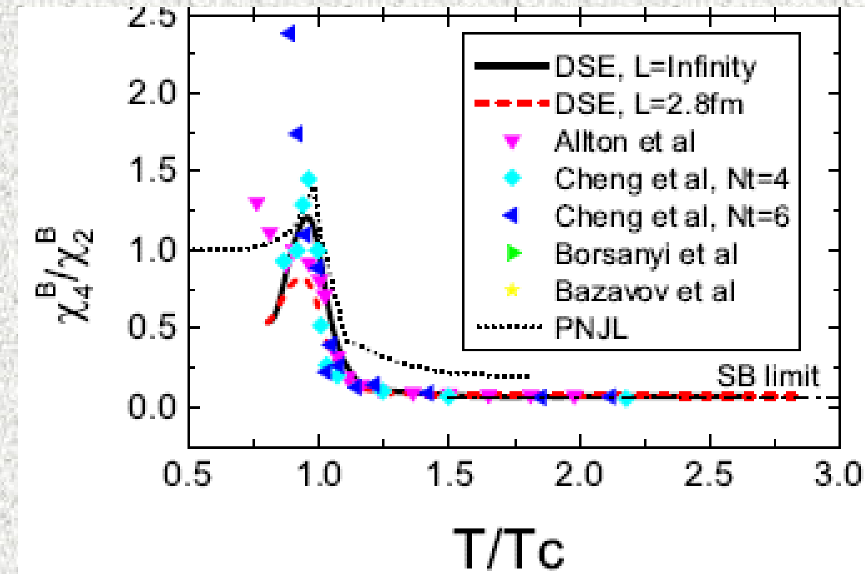

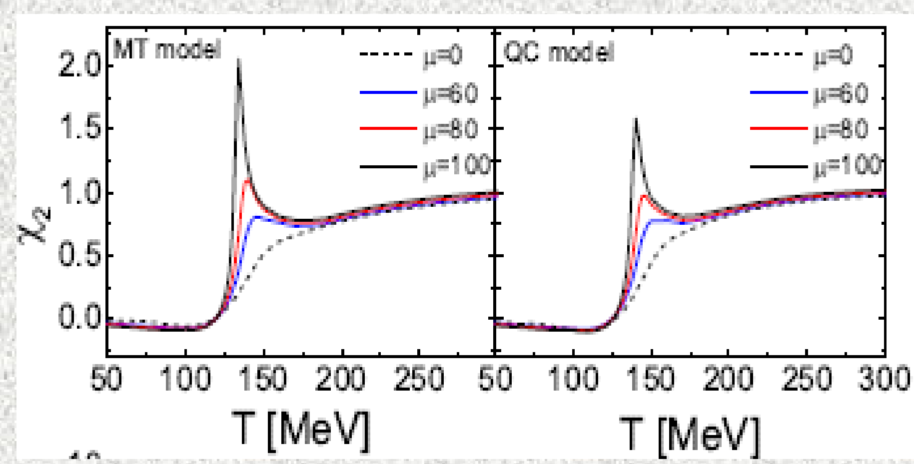

X.Y. Xin, S.X. Qin, YXL, PRD 90, 076006 (2014)

✦ Quark Number Density Fluctuations vs μ in the DSE

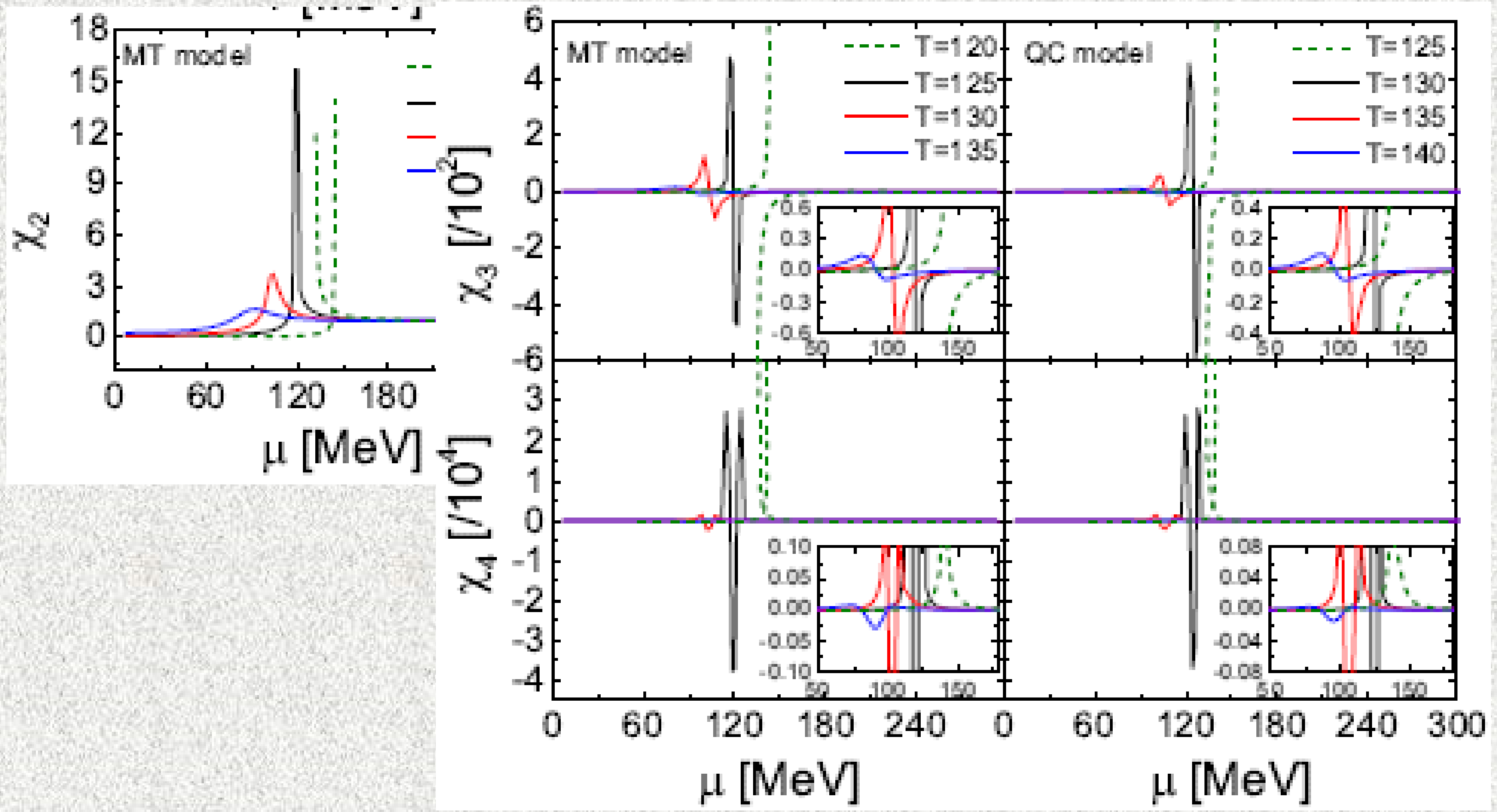

W. J. Fu, Y. X. Liu, and Y. L. Wu, Phys. Rev. D **81**, 014028 (2010);
X.Y. Xin, S.X. Qin, YXL, Phys. Rev. D 90, 076006 (2014)

✦ Quark Number Density Fluctuations vs μ in the DSE

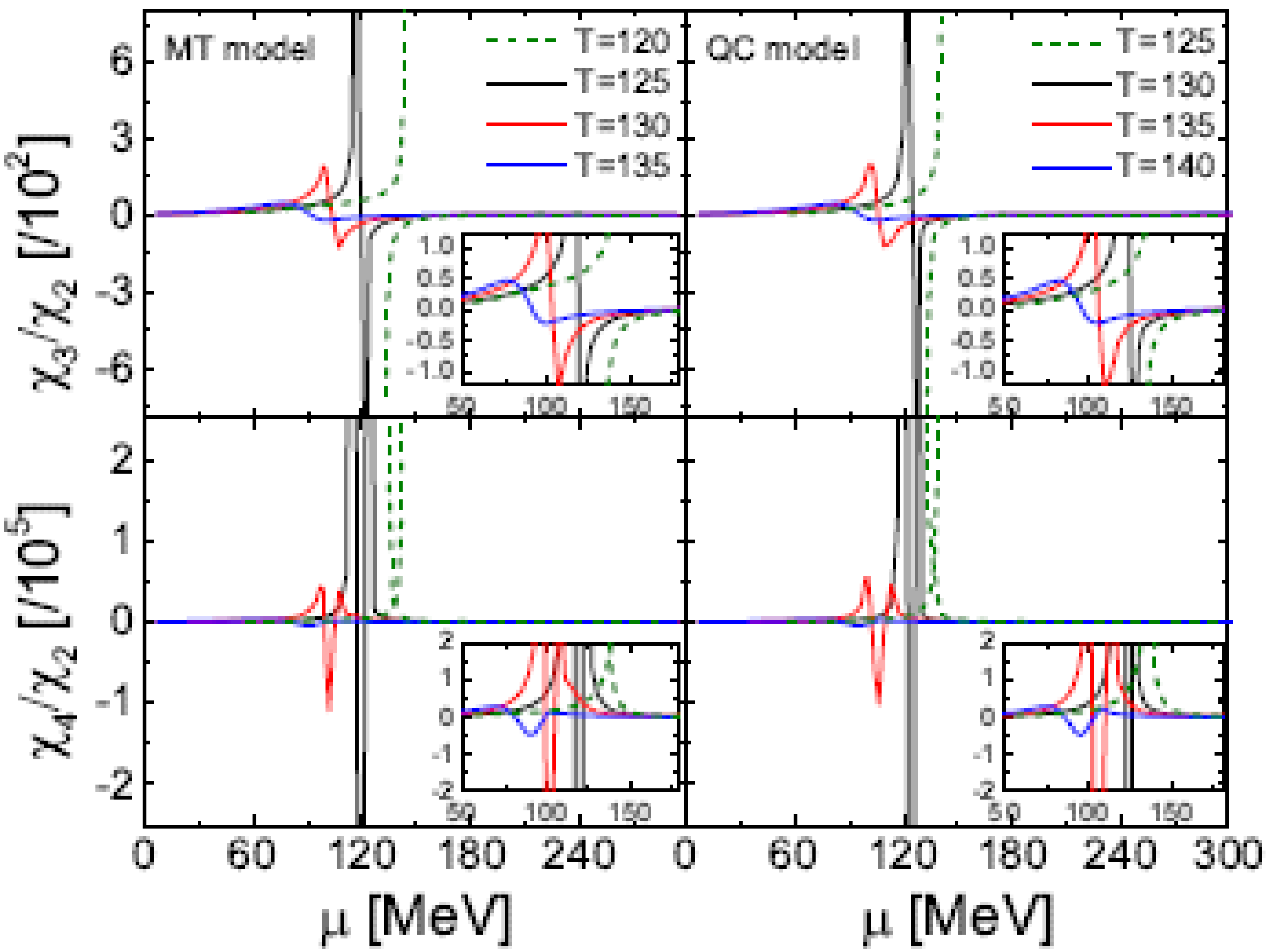

In crossover region, the fluctuations oscillate obviously;

In 1st transt., overlaps exist.

At CEP, they diverge!

W. J. Fu, Y. X. Liu, and Y. L. Wu, PRD **81**, 014028 (2010);
X.Y. Xin, S.X. Qin, YXL, Phys. Rev. D 90, 076006 (2014)

✦ Flavor dependence of the QN Density Fluctuations vs T in the DSE

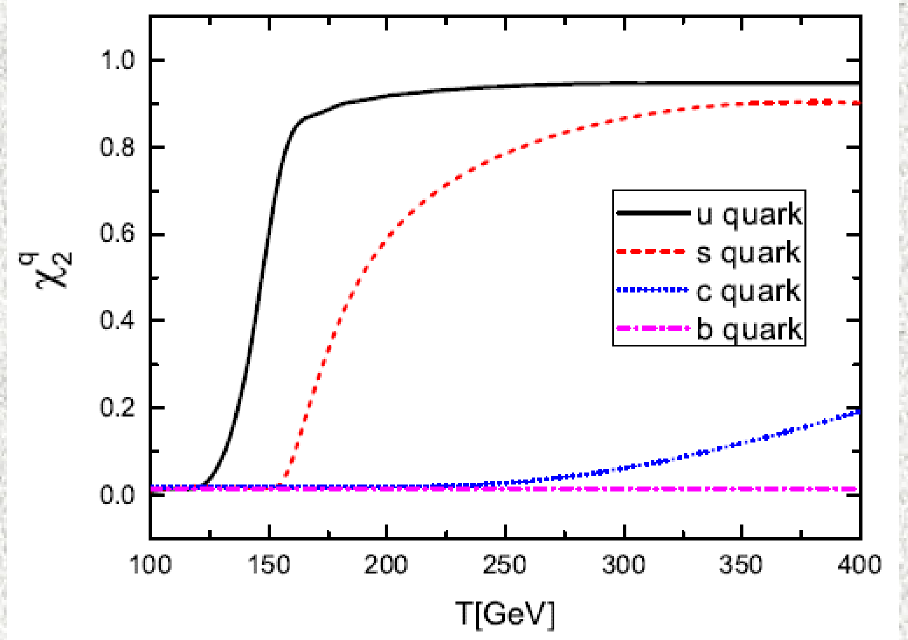

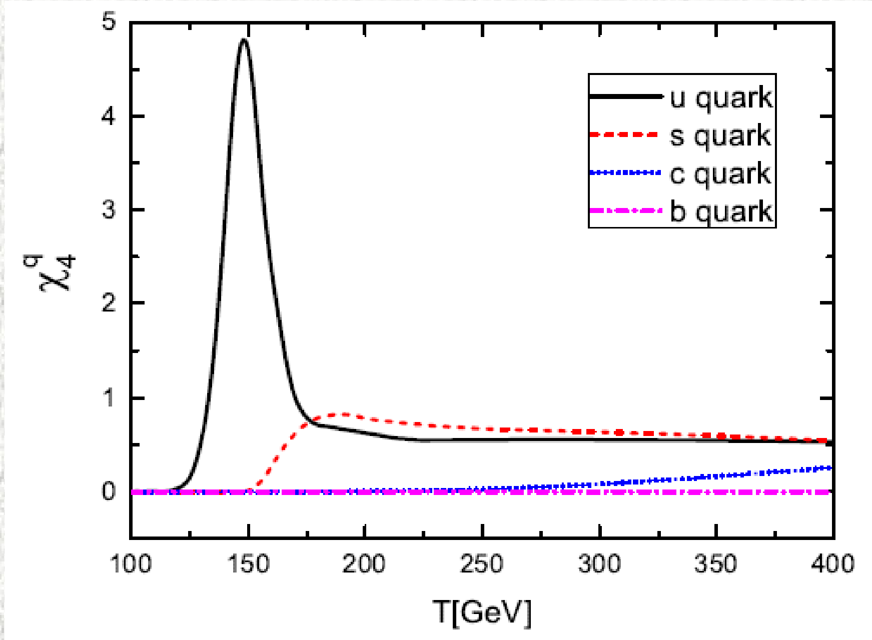

The fluctuations of heavy flavor quarks are much Smaller than those of the light flavors.

Net-proton fluctuations are good approx. baryon F.

Jing Chen, Y. X. Liu, et al., to be published.

✦ Relating with Experiment Directly

Chemical Freeze out Conditions

Fitting the Expt. data of χ_1^B / χ_2^B & χ_3^B / χ_1^B ,

$L = \infty$

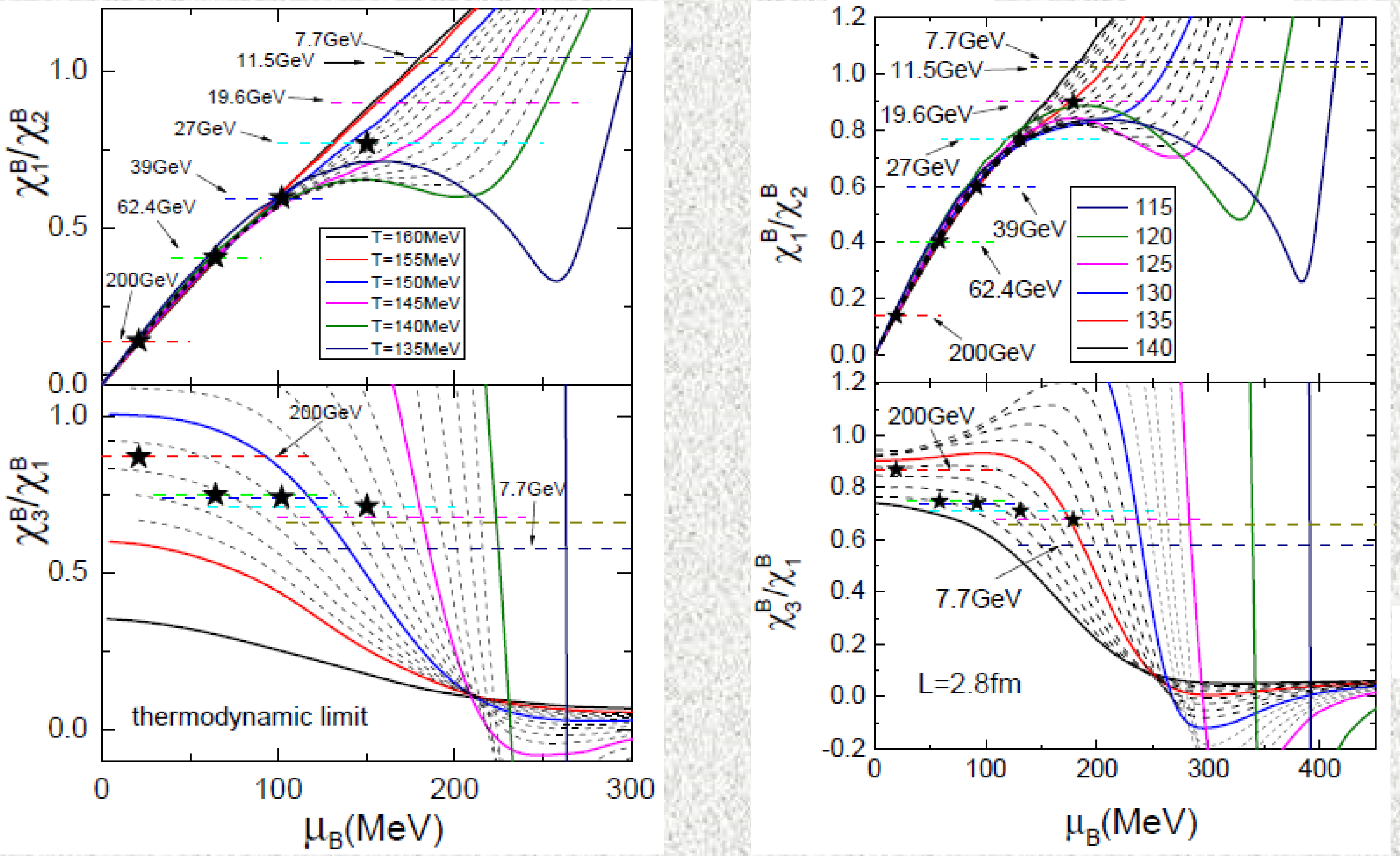

$L = 2.8\,fm$

We get the T & μ_B of the chemical freeze-out states, in turn, the collision energy dependence of the CFO cond.

✦ Relating with Experiment Directly

Chemical Freeze out Conditions

$$\mu_B^f = \frac{c}{1+d\sqrt{S_{NN}}}\,, \qquad T^f = T^0\left[1 - a\left(\frac{\mu_B^f}{T^0}\right)^2 - b\left(\frac{\mu_B^f}{T^0}\right)^4\right].$$

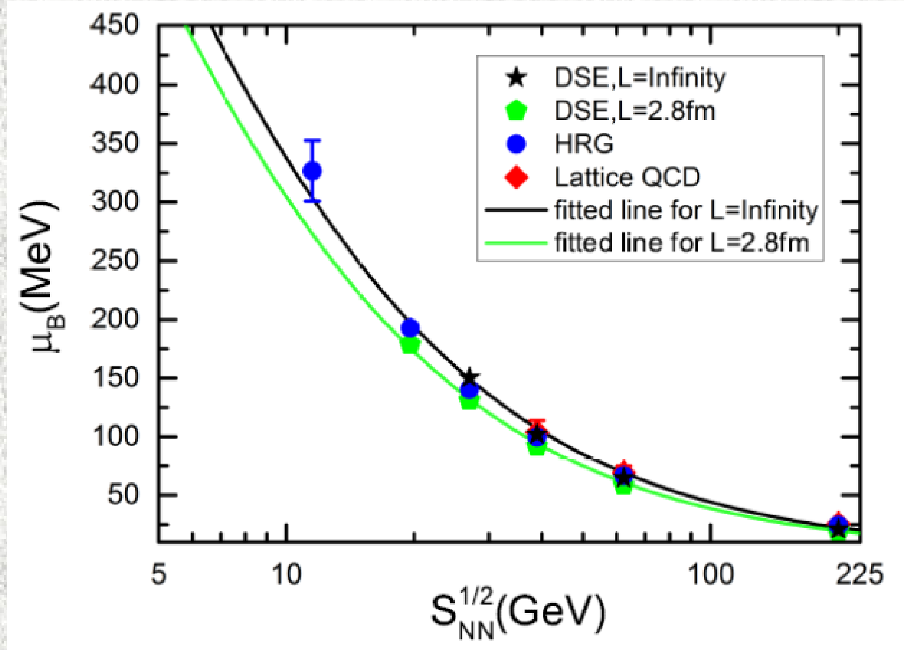

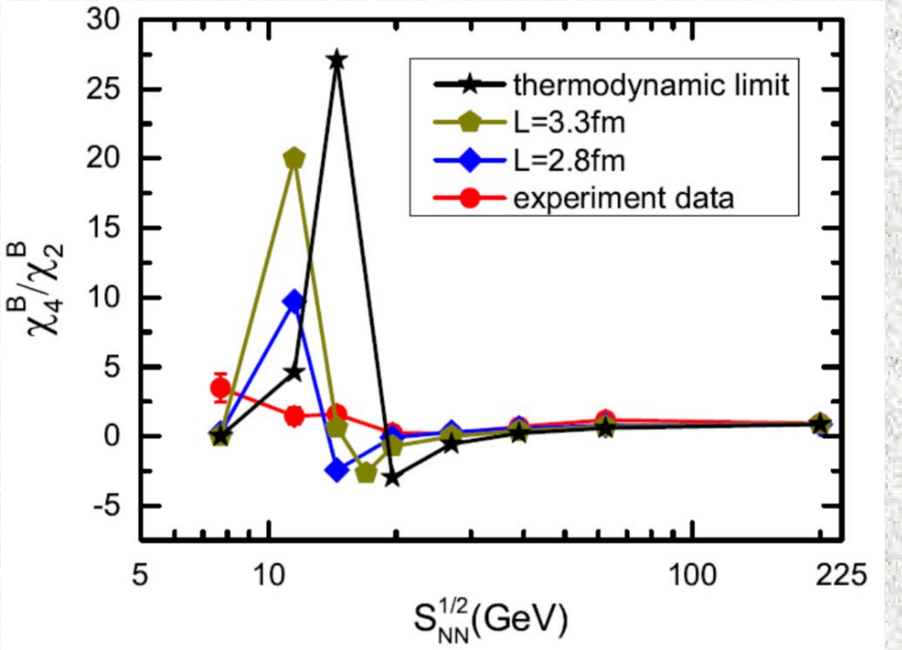

FRG calculations of Wei-jie & Jan (PRD 92,116006 ('15); PRD 93, 091501(R) ('16), etc) also describe the data in $\sqrt{S_{NN}} \geq 19.6$ GeV region excellently.

Jing Chen, Fei Gao, Yu-xin Liu, arXiv: 1510.07543.

♠ A significant issue: finite size effects

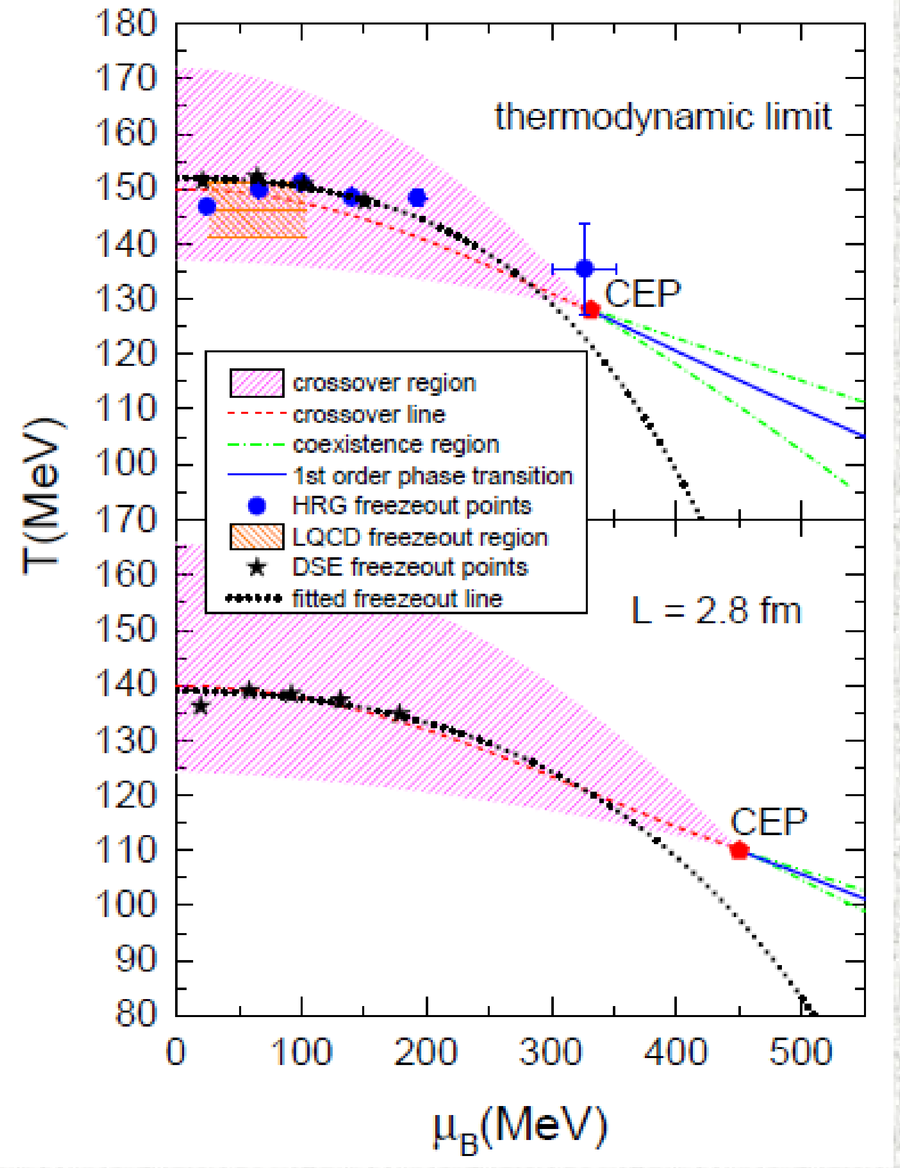

Thermodynamical Limit:

T_c (μ = 0) = 150 MeV,

T_f (μ = 0) = 151 MeV,

T_{CEP} = 128 MeV,

$\mu^B{}_{CEP}$ = 330 MeV;

***L* = 2.8 fm case:**

T_c (μ = 0) = 140 MeV,

T_f (μ = 0) = 139 MeV,

T_{CEP} = 109 MeV,

$\mu^B{}_{CEP}$ = 450 MeV;

Jing Chen, Fei Gao, YXL, et al., to be published.

♠ Different methods give distinct locations of the CEP arises from diff. Conf. Length

Model	$(D\omega)^{1/3}$	ω	T_c	(μ_E^q, T_E)	μ_E^q/T_E
	0.72	0.40	0.146	(0.120,0.124)	0.97
MT	0.72	0.45	0.132	(0.220,0.098)	2.24
	0.72	0.50	0.124	(0.281,0.070)	4.01
	0.80	0.40	0.173	(0.075,0.165)	0.45
QC	0.80	0.50	0.150	(0.124,0.129)	0.96
	0.80	0.60	0.131	(0.201,0.099)	2.03

Small ω → long range in coordinate space

MN model → infinite range in r-space

NJL model → "zero" range in r-space

Longer range Int. → Smaller μ_E/T_E

S.X. Qin, YXL, et al, PRL106,172301('11); X. Xin, S. Qin, YXL, PRD90,076006

V. Summary & Remarks

♠ Introduced the DSE of QCD briefly

- Dynamical mass generation — DCSB;
- Confinement — Positivity violation of SDF;
- Hadron mass, decay, structure;

♠ Discussed criteria of the PTs & PDs in DSE

- critical exponents, $(T_E, \mu_{B,E})_{TL} = (128, 333)$ **MeV**;
- susceptibilities, $(T_E, \mu_{B,E})_{TL} \cong (128, 330)$ **MeV**;
- BN Fluctuations, $(T_E, \mu_{B,E})_{TL} \cong (128, 330)$ **MeV**.

♠ DSE approach is quite promising !

Thanks !!

♠ Property of the matter above but near the T_c

Solving quark's DSE → Quark's Propagator

In M-Space, only Yuan, Liu, etc, PRD 81, 114022 (2010).

Usually in E-Space, Analytical continuation is required.

Maximum Entropy Method

(Asakawa, et al., PPNP 46,459 (2001); Nickel, Ann. Phys. 322, 1949 (2007))

→ **Spectral Function**

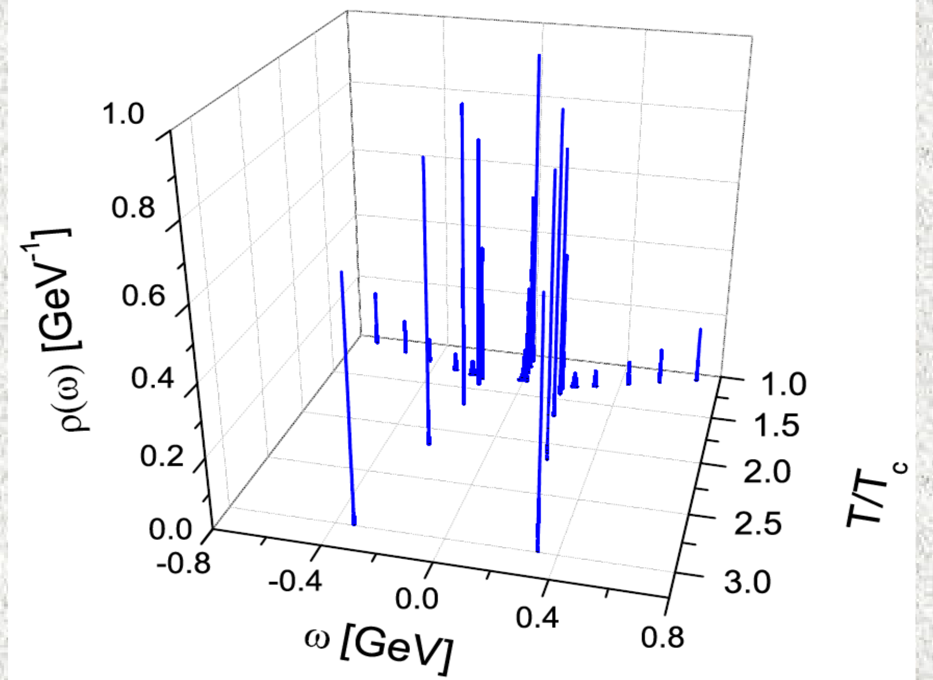

Qin, Chang, Liu, et al., PRD 84, 014017(2011)

Disperse Relation and Momentum Dependence of the Residues of the Quasi-particles' poles

$T = 3.0T_C$ **$T = 1.1T_C$**

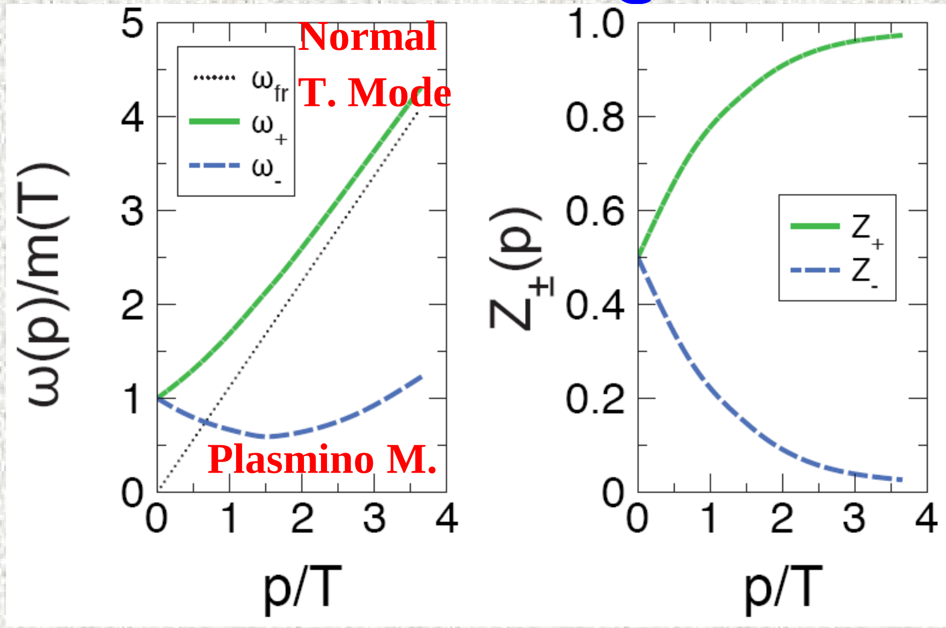

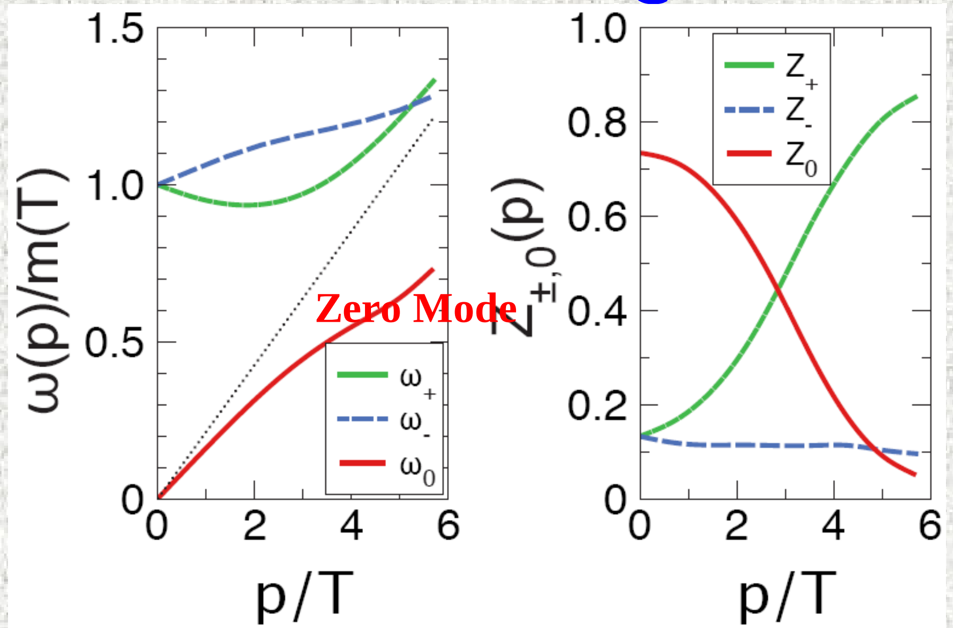

- ♣ **The zero mode exists at low momentum ($<7.0T_C$), and is long-range correlation ($\lambda \sim \omega^{-1} > \lambda_{FP}$) .**
- ♣ **The quark at the *T* where DCS has been restored involves still rich phases. And the matter is sQGP.**

S.X. Qin, L. Chang, Y.X. Liu, et al., Phys. Rev. D 84, 014017(2011);
F. Gao, S.X. Qin, Y.X. Liu, et al., Phys. Rev. D 89, 076009 (2014).

♠ Consistence with Thermodynamic Evolution

$$S = -\partial(\Omega/V)/\partial T$$
$$= -\int \frac{d^4k}{(2\pi)^4}\frac{\partial n(\omega)}{\partial T}\,\mathrm{Im}\log D^{-1}(\omega,k)$$
$$+\int \frac{d^4k}{(2\pi)^4}\frac{\partial n(\omega)}{\partial T}\,\mathrm{Im}\Pi(\omega,k)\,\mathrm{Re}D(\omega,k) + S'$$

Crossover Region

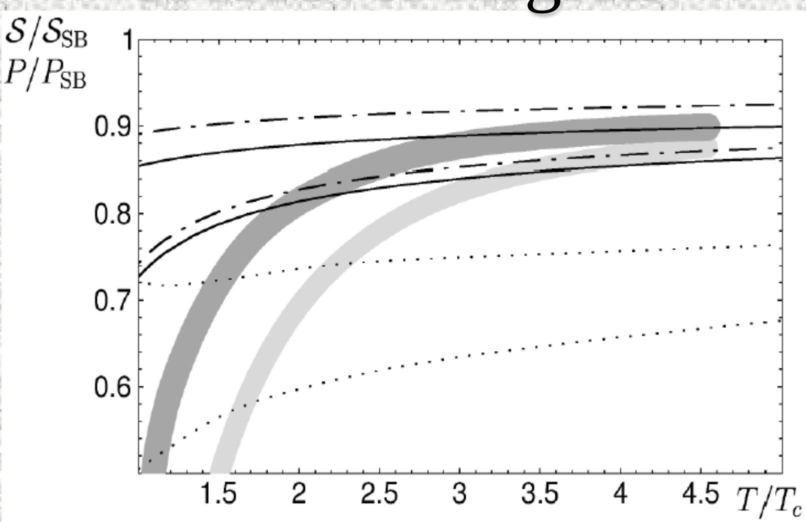

J.-P. Blaizot, et al., PRL 83, 2906

First Order Region

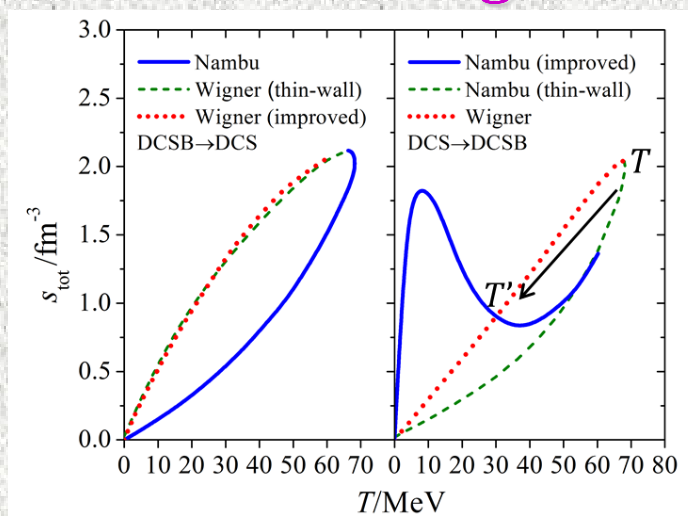

柯伟尧, et al., PRD 89, 074041('14),
高飞, et al., PRD 94, 094030 (2016)

Chiral Symmetry Breaking generates the Anomalous Magnetic Moment of Quark

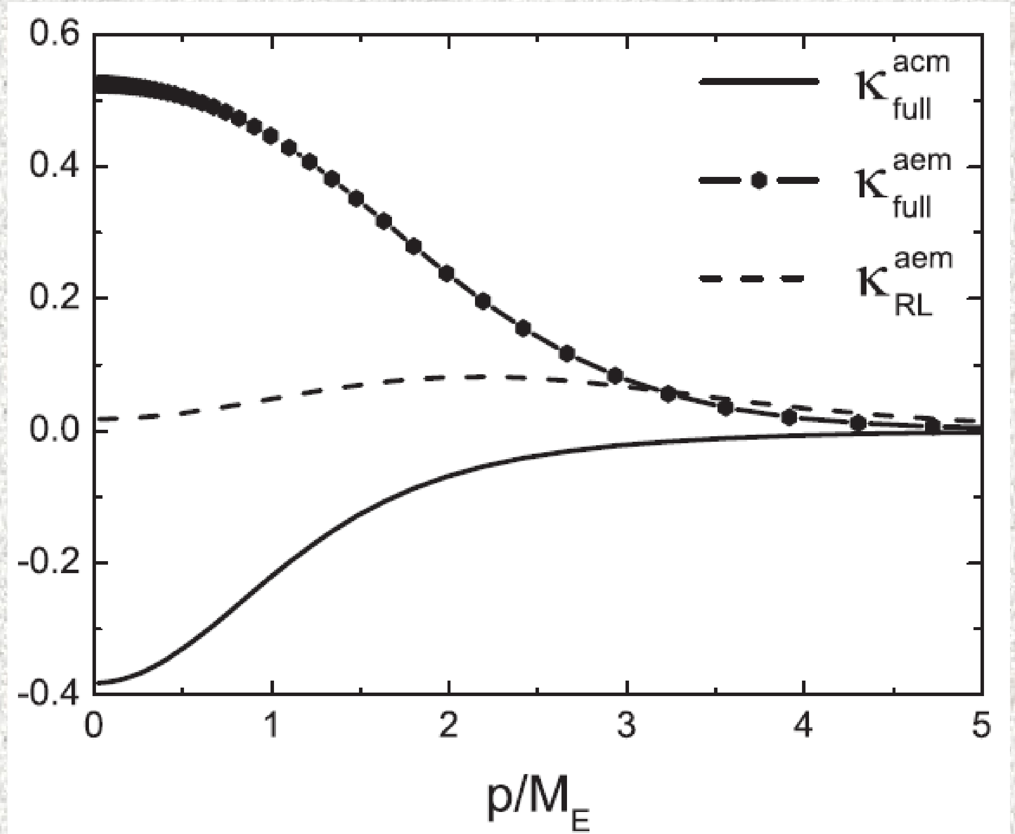

Consequently, nucleon has anomalous magnetic moment.

L. Chang, Y.X. Liu, & C.D. Roberts, PRL 106, 072001 (‘11)

♠ Density & Temperature Dependence of some Properties of Nucleon in DSE Soliton Model

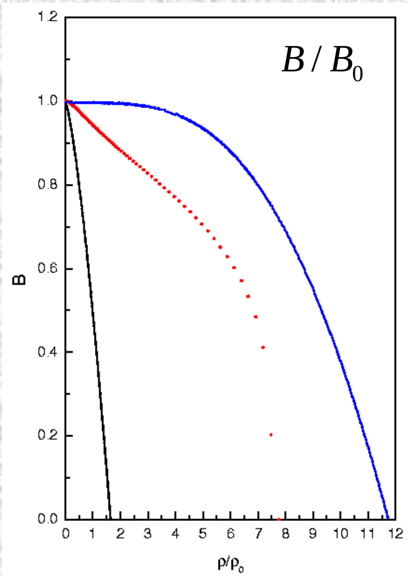

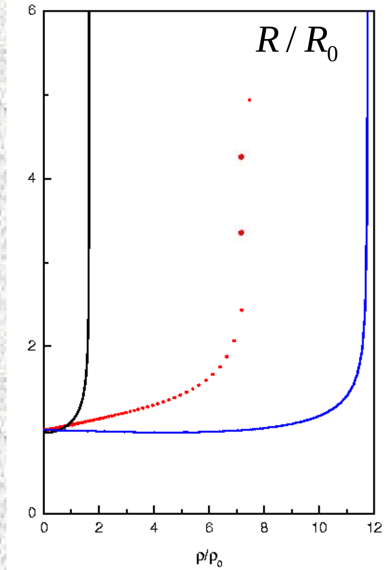

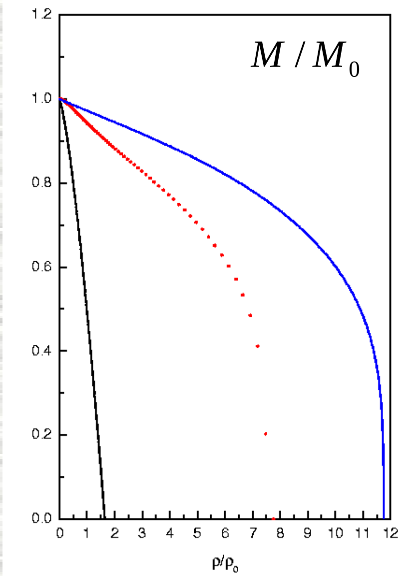

Y. X. Liu, et al., NP A 695, 353 (2001); NPA 725, 127 (2003); NPA 750, 324 (2005))

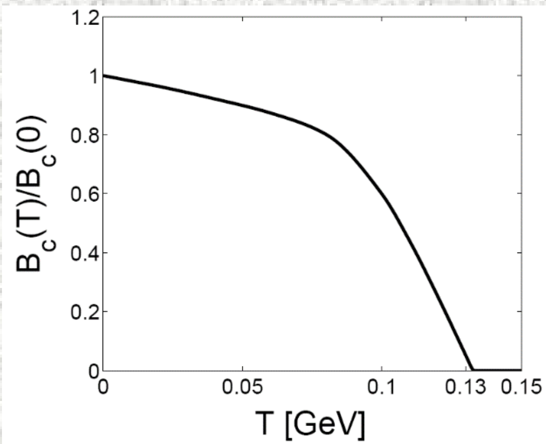

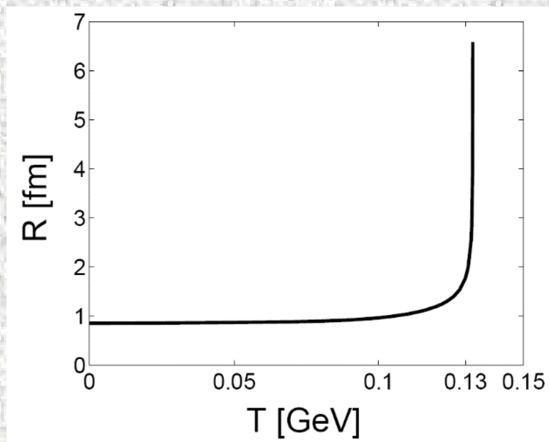

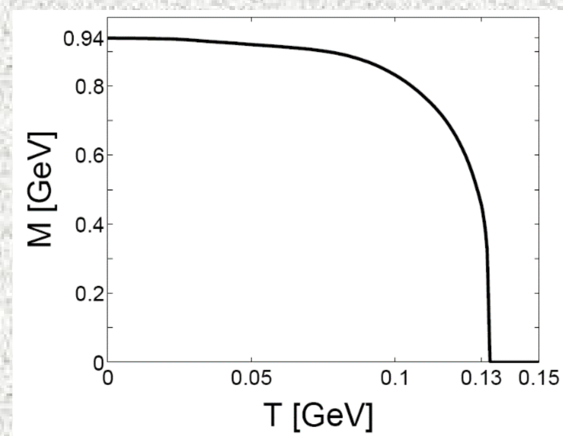

(Y. Mo, S.X. Qin, and Y.X. Liu, Phys. Rev. C 82, 025206 (2010))

♠ Key Issue 2: Interface effects

- Interface tension between the DCS-unconf. phase and the DCSB-confined phase

With the scheme (J. Randrup, PRC 79, 054911 (2009))

$$F(\vec{r}) = n\mu + \tfrac{1}{2}C(\nabla n)^2 + \cdots\cdots \cong n\mu + \tfrac{1}{2}C(\nabla n)^2,$$

we have $\Delta F_T = F_T(n) - F_M(n),$

with $F_M(n) = F_T(n_L) + \frac{F_T(n_H) - F_T(n_L)}{n_H - n_L}(n - n_L)$

and (EoM) $\Delta F_T + \tfrac{1}{2}C(\tfrac{\partial n}{\partial r})^2 = 0$.

$$\rightarrow \quad \gamma(T) = \int_{-\infty}^{+\infty} \Delta F_T \, dx = -\tfrac{1}{2}\int_{-\infty}^{+\infty} C(\tfrac{\partial n}{\partial r})^2 dx,$$

$$= \int_{n_L}^{n_H} \sqrt{\tfrac{C}{2}\Delta F_T(n)}\, dn$$

- **Interface tension between the DCS-unconf. phase and the DCSB-confined phase**

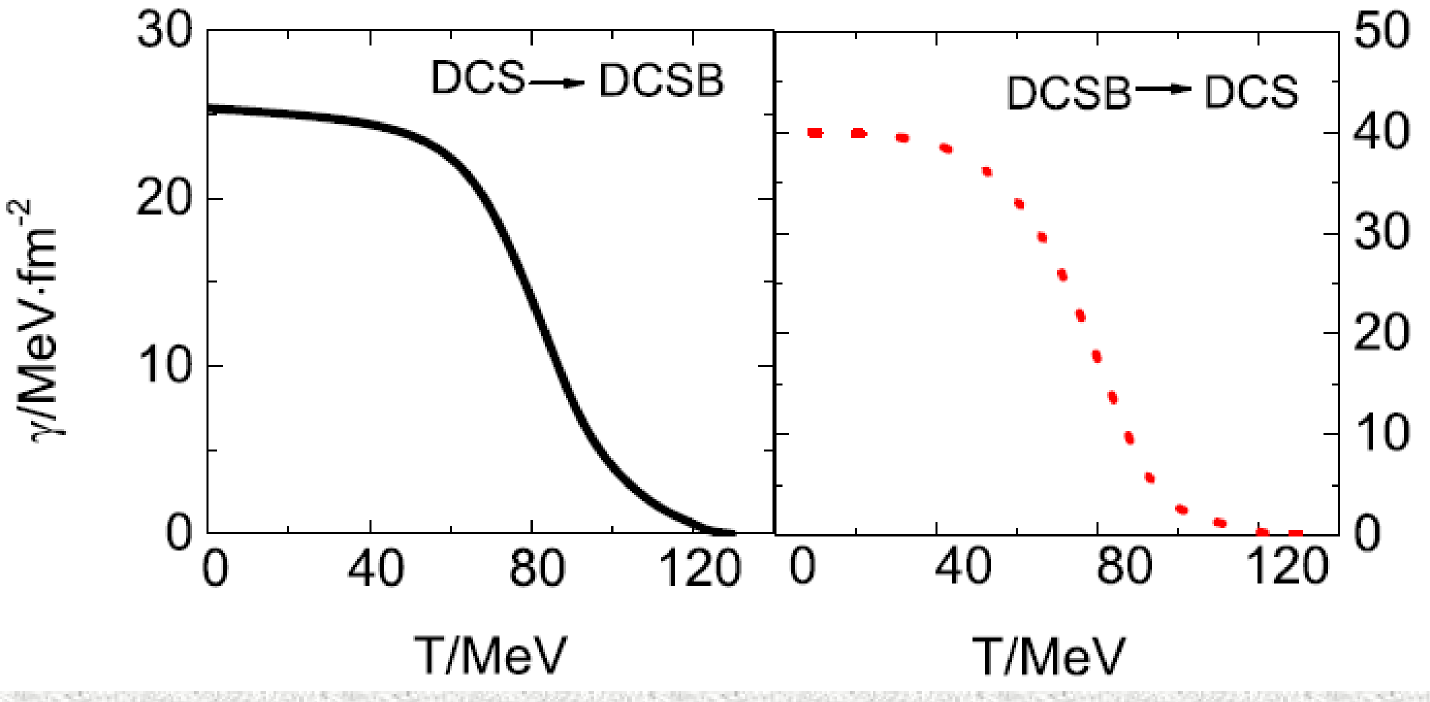

Parameterized as $\gamma(T) = a + be^{(c/T + d/T^2)}$,

with parameters

	$a/(\mathrm{MeV/fm^2})$	$b/(\mathrm{MeV/fm^2})$	$c/$ MeV	$d/\mathrm{GeV^2}$
DCS → DCSB	25.4	−1.5	736	−0.048
DCSB → DCS	40.0	−8.1	399	−0.025

Fei Gao, & Yu-xin Liu， Phys. Rev. D 94, 094030 (2016)

- **Effects of the Interface**

e.g., **Solving the entropy puzzle**

In thermodynamical limit

$$s_V = \frac{1}{T}(\epsilon + P - \mu n) = \frac{\partial P}{\partial T}.$$

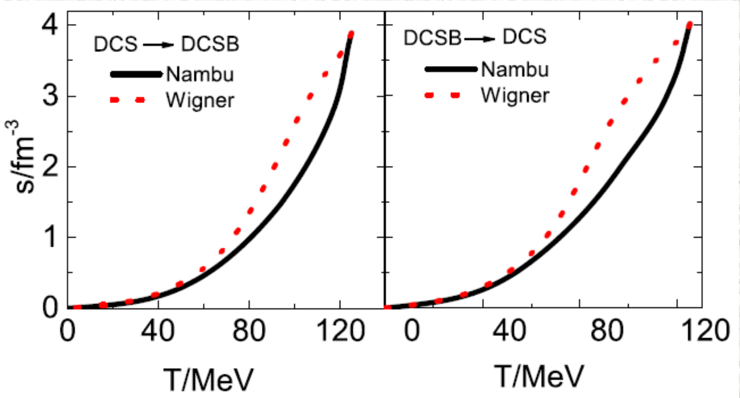

With the interface entropy density

$$s_A = -\left(\frac{\partial \gamma}{\partial T}\right)_{VA}$$

being included, we have

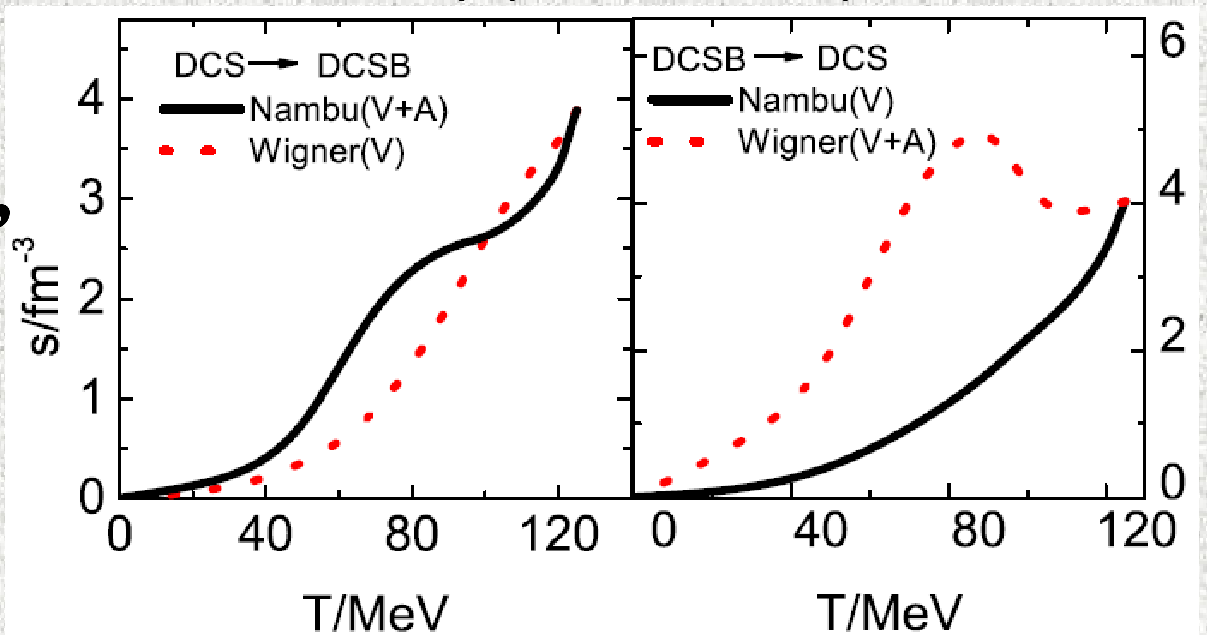

Fei Gao, & Y.X. Liu, Phys. Rev. D 94, 094030 (2016)

●●●●●●

III. Thermal Properties

♠ Basic Formulae & Algorithm:

Pressure

$$P[S] = \frac{T}{V} lnZ = \frac{T}{V}\left(TrLn[\beta S^{-1}] - \frac{1}{2} Tr[\Sigma S]\right),$$

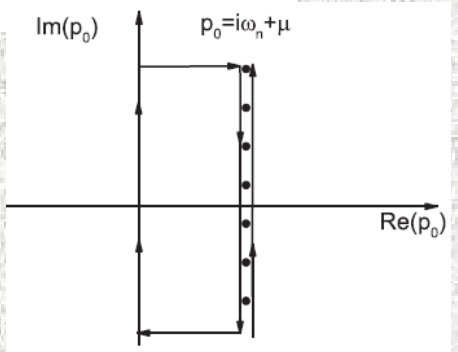

Entropy Density $s(T) = \partial P[S] / \partial T$,

Energy Density $\varepsilon = -P + Ts$,

Sound Speed $c_s^2 = \dfrac{\partial P}{\partial \varepsilon}$,

Heat capability & latent heat

$$c_V = T\frac{\partial s}{\partial T}\,, \quad L = T\Delta s = \Delta\varepsilon - \mu\Delta\rho\,.$$

♠ Trace Anomaly at Zero Chemical Potential

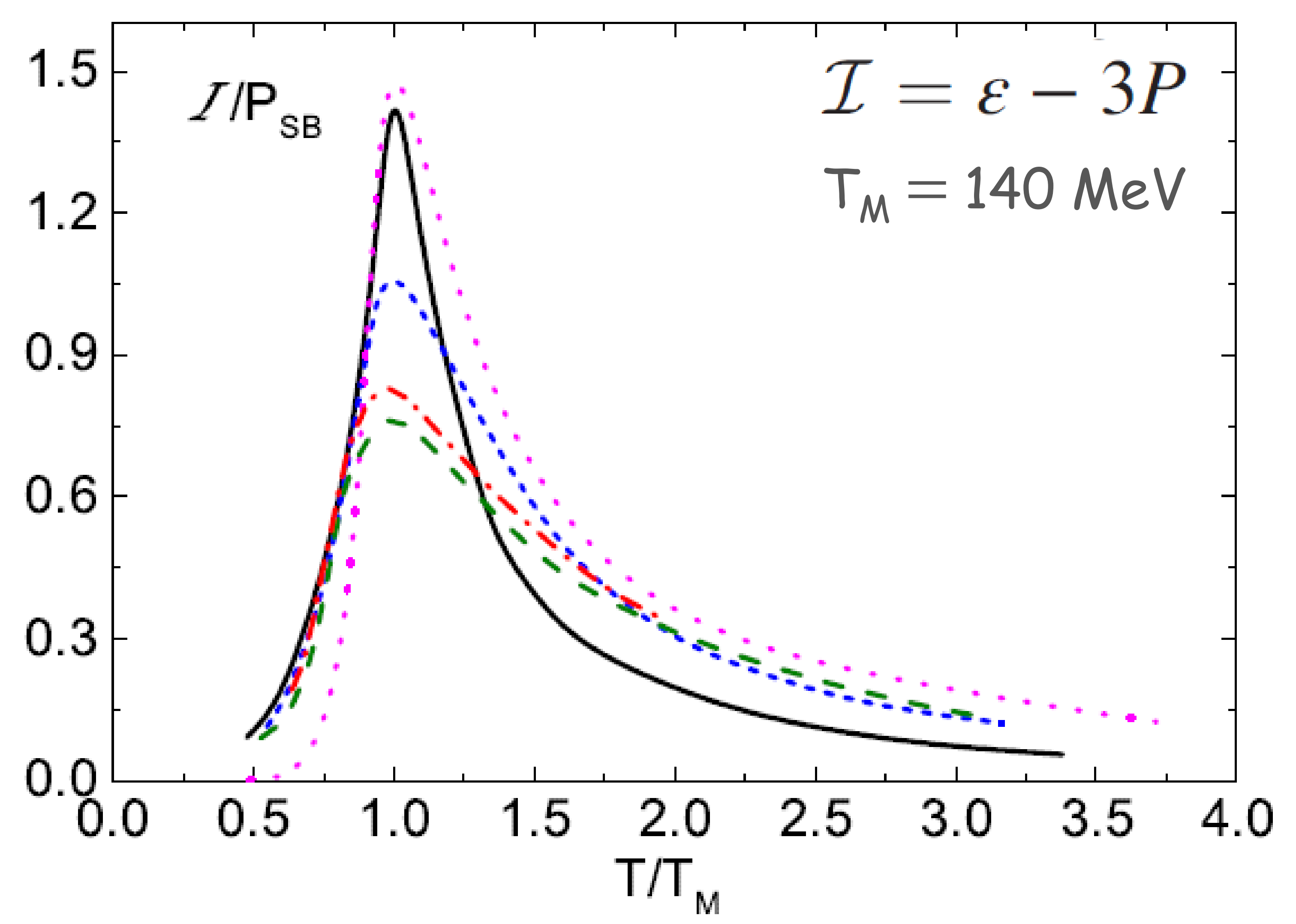

Gao, Chen, Liu, Qin, Roberts, Schmidt, Phys. Rev. D 93, 094019 (2016).

♠ Pressure & Trace Anomaly at Non-Zero Chemical Potential

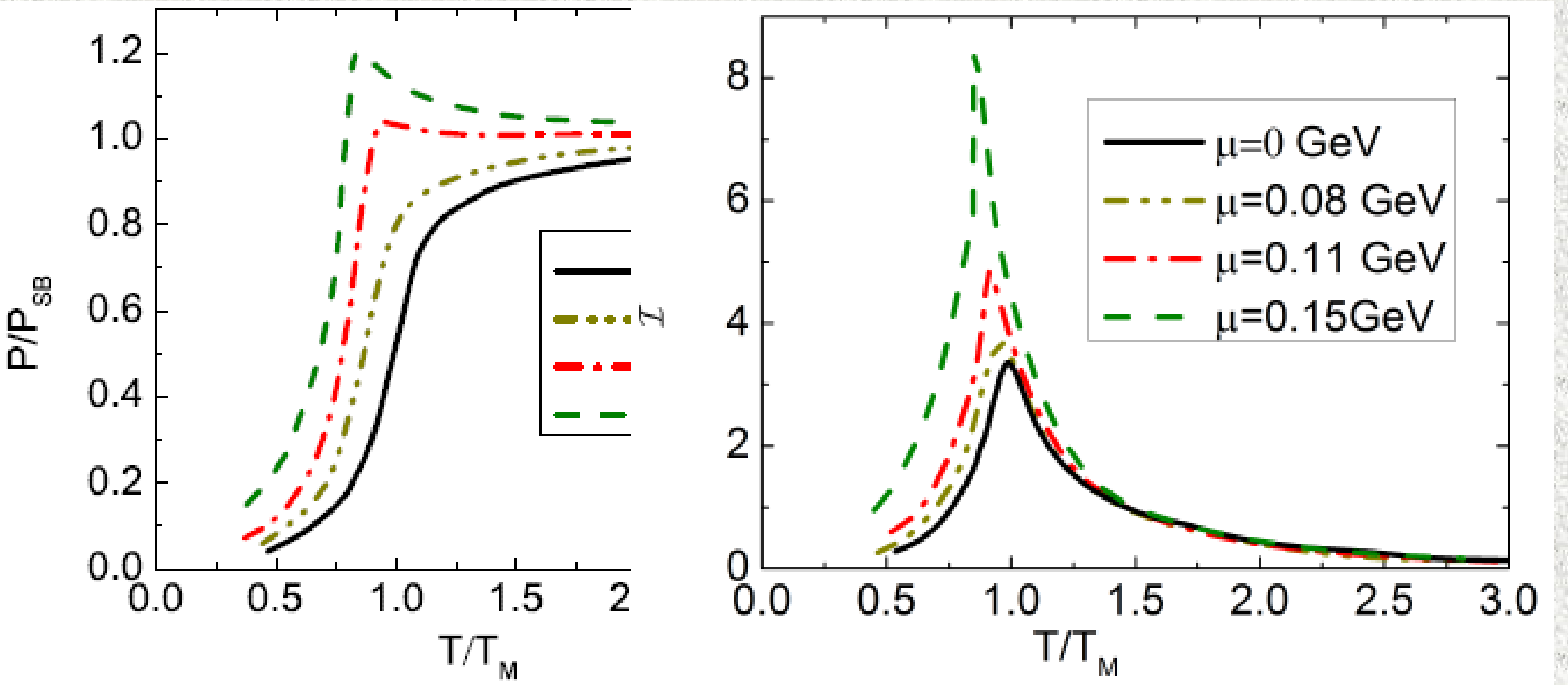

T_M = 140 MeV

Gao, Chen, Liu, Qin, Roberts, Schmidt, Phys. Rev. D 93, 094019 (2016).

♠ Sound Speed squared

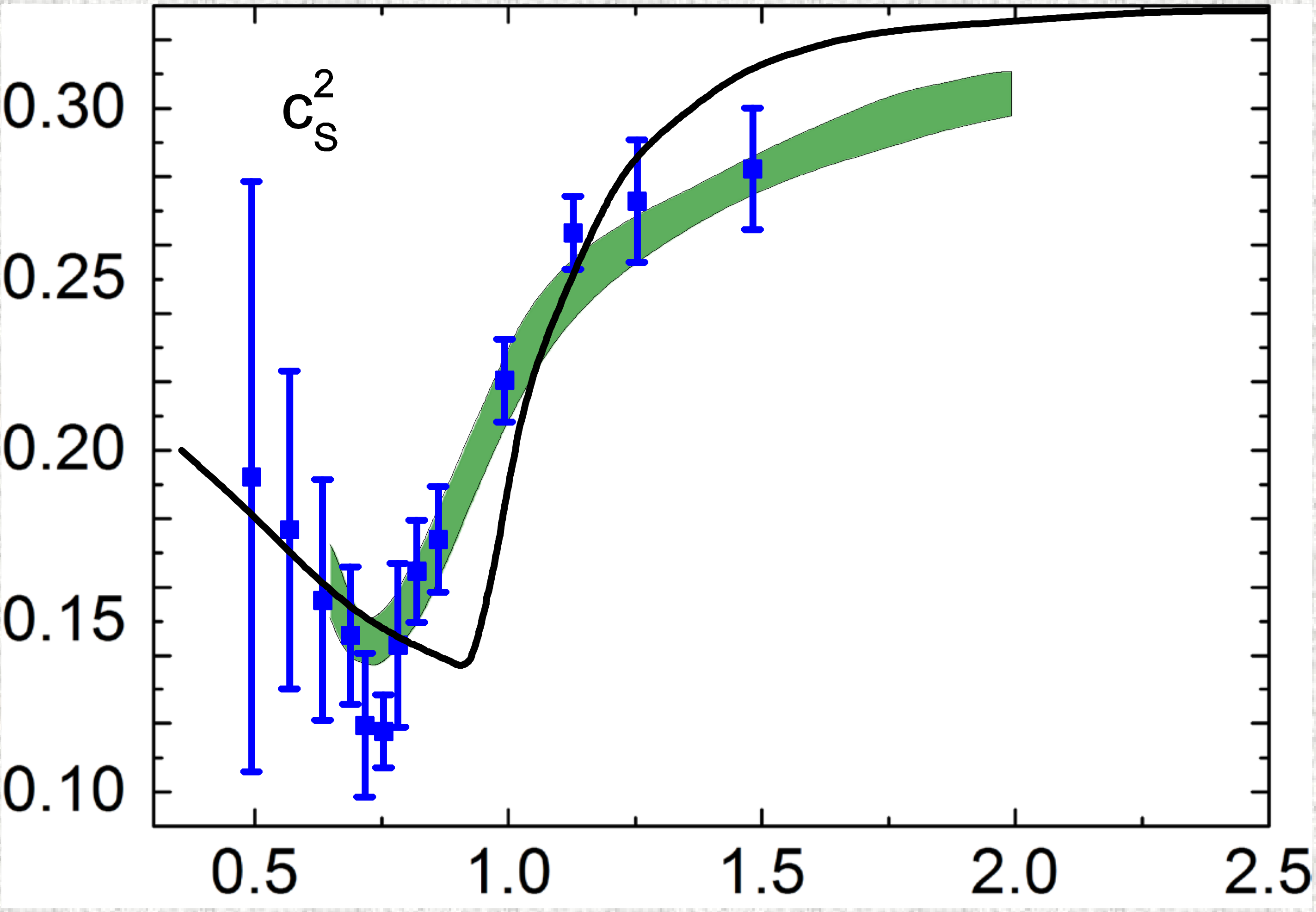

T_M = 140 MeV

Gao, Chen, Liu, Qin, Roberts, Schmidt, Phys. Rev. D 93, 094019 (2016).

♠ Specific heat capability & Latent heat

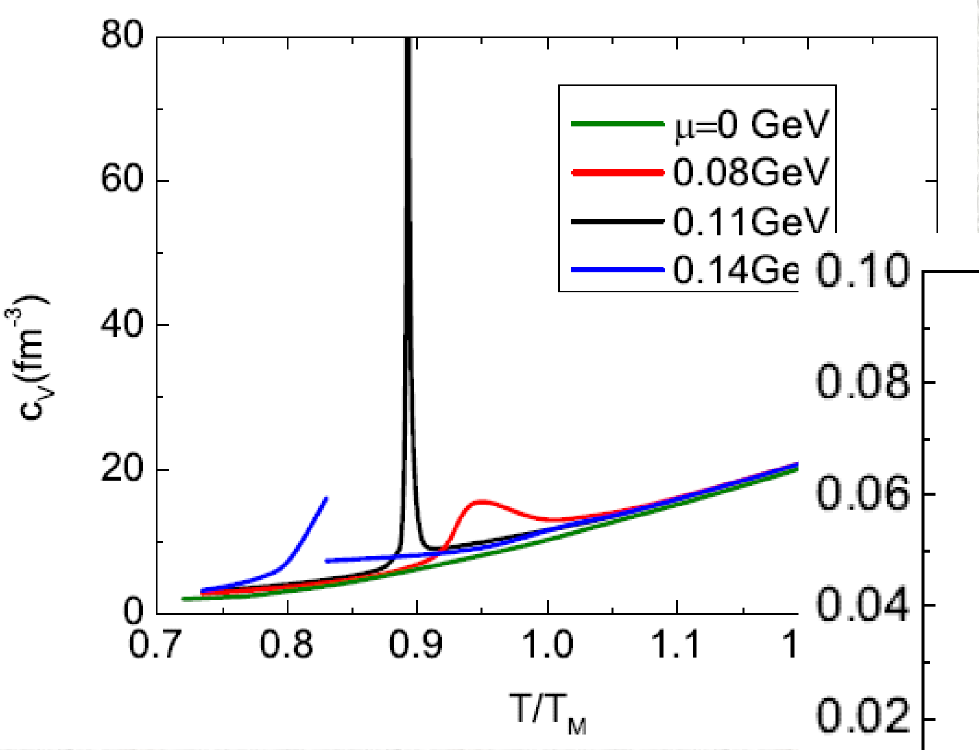

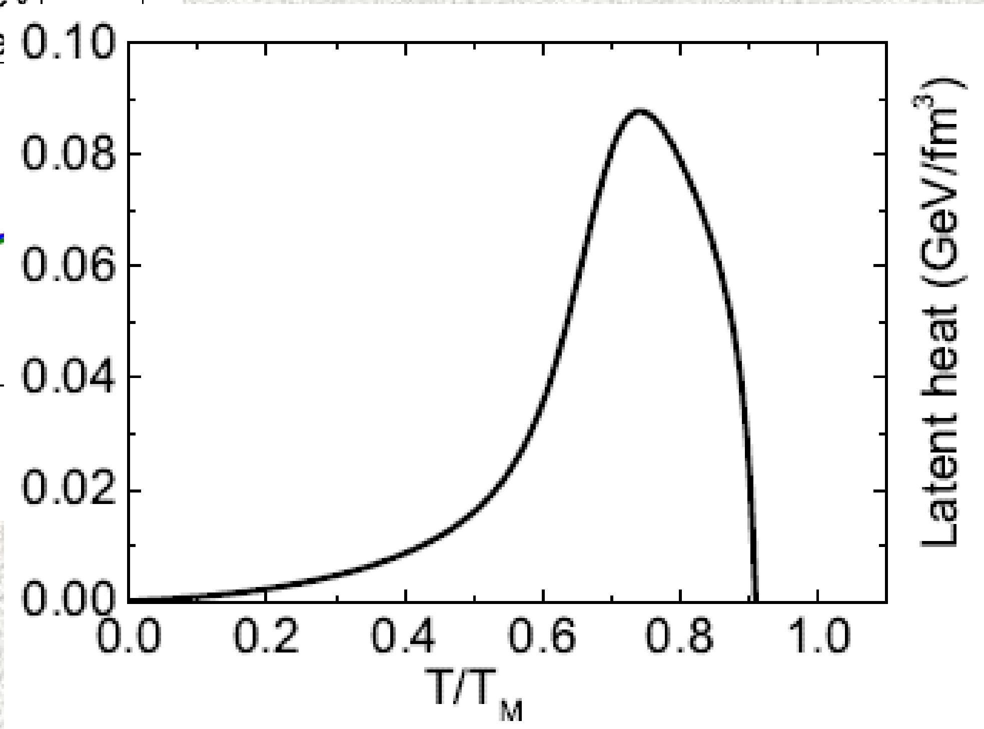

T_M = 140 MeV

Gao, Chen, Liu, Qin, Roberts, Schmidt, Phys. Rev. D 93, 094019 (2016).

♠ Entropy

Only the Uniform Part

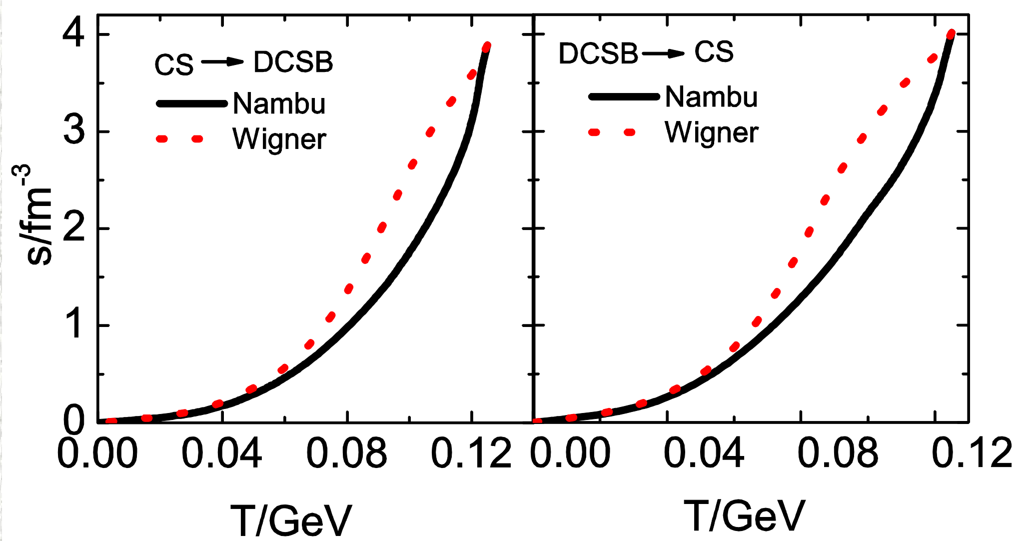

Entropy puzzle !

Including the surface Part with

$$s_A = -\frac{\partial \gamma}{\partial T}$$

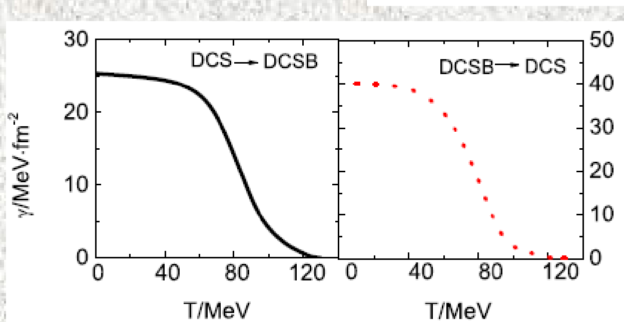

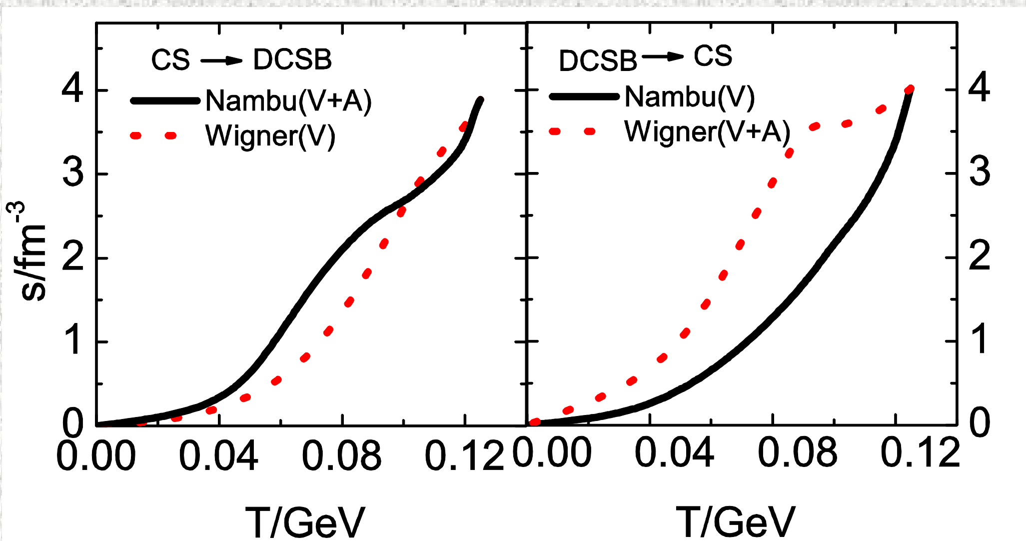

Fei Gao, Y.X. Liu, Phys. Rev. D 94, 094030 (2016)

♠ An Astronomical Observable: Gravitational Mode Oscillation Frequency

- **G-Wave in Binary Neutron Star Merger**

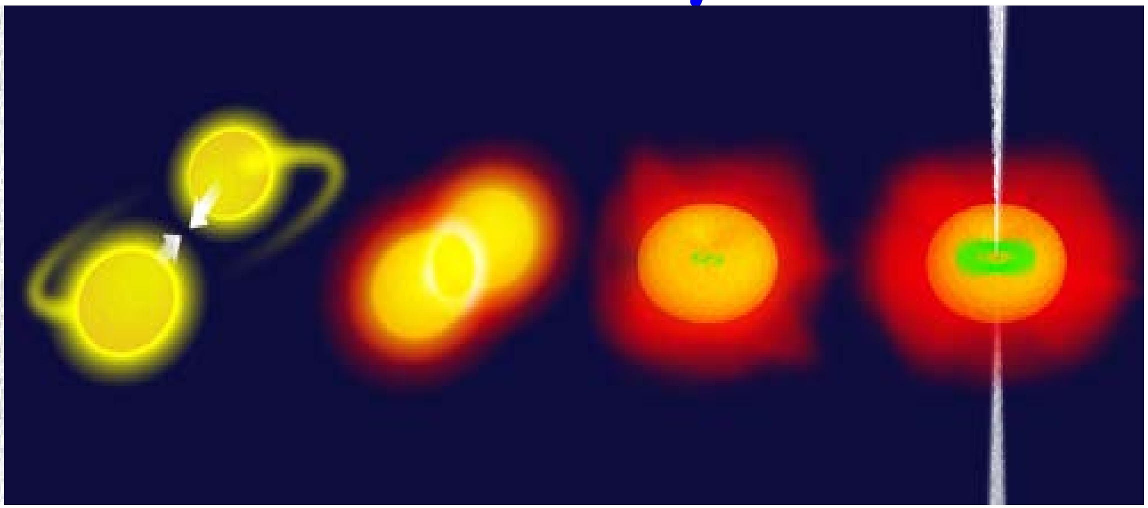

$F_{\text{postmerger}} \in (1.84, 3.73)\,\text{kHz}$, with width<200Hz, (PRD 86, 063001(2012))

$F_{\text{spiral}} < F_{\text{postmerger}}$

- **G-Wave in Newly Born Compact Star (NS, QS)**

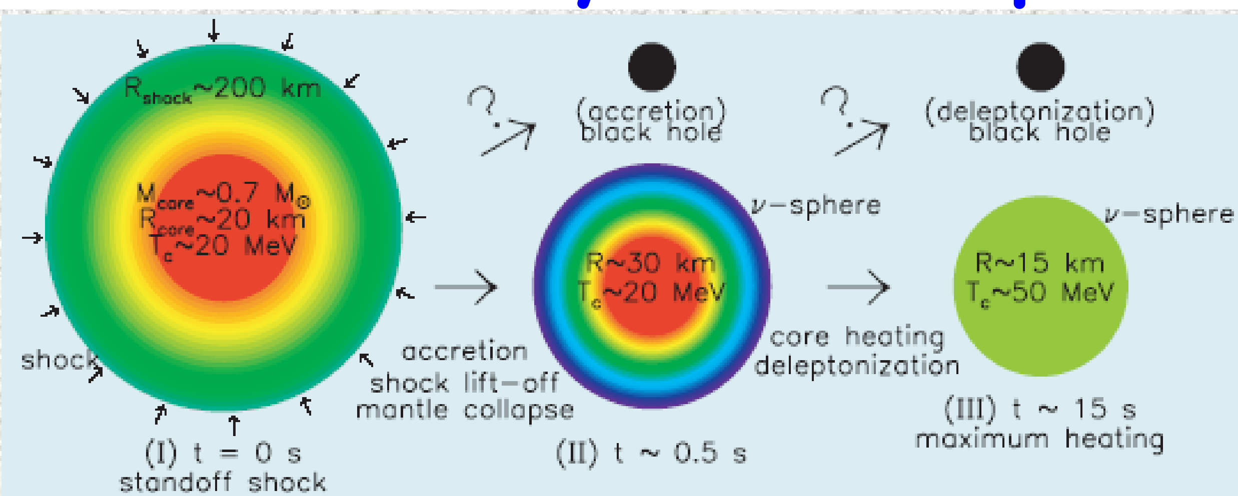

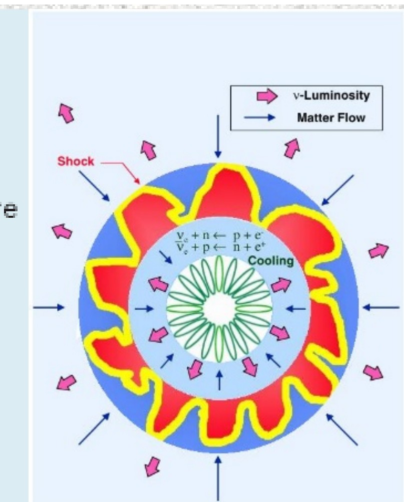

- Comparison of G-mode Oscillation Frequencies of the two kind nb Stars

Neutron Star: RMF, Quark Star: Bag Model

→ Frequency of the G-mode oscillation

Radial order of g-mode	Neutron Star			Strange Quark Star		
	$t=100$	$t=200$	$t=300$	$t=100$	$t=200$	$t=300$
$n=1$	717.6	774.6	780.3	82.3	78.0	63.1
$n=2$	443.5	467.3	464.2	52.6	45.5	40.0
$n=3$	323.8	339.0	337.5	35.3	30.8	27.8

W.J. Fu, H.Q. Wei, and Y.X. Liu, arXiv: 0810.1084, Phys. Rev. Lett. 101, 181102 (2008)

• Comparison with other modes

Neutron Star: RMF, Quark Star: Bag Model

→ Frequencies of the f- & p-mode oscillations

Modes	Neutron Star			Strange Quark Star		
	$t=100$	$t=200$	$t=300$	$t=100$	$t=200$	$t=300$
${}_2f$	1103	1133	1176	2980	2997	3016
${}_2p_1$	2265	2426	2494	18282	17330	16792
${}_2p_2$	3780	4054	4179	28792	27288	26438
${}_2p_3$	5319	5702	5869	38988	36950	35798

♣ G-mode oscillation in quark star has very low freq. !

W.J. Fu, Z. Bai, Y.X. Liu, arXve:1701.00418

- **Taking into account the DCSB effect**

Newly obtained results for QS in NJL Model

Radial order of g-mode	Neutron Star			Strange Quark Star		
	$t=100$	$t=200$	$t=300$	$t=100$	$t=200$	$t=300$
$n=1$	717.6	774.6	780.3	100.2	115.4	107.4
$n=2$	443.5	467.3	464.2	60.1	57.0	51.8
$n=3$	323.8	339.0	337.5	42.9	40.9	40.2

- **Work in the DS equation scheme is under progress. (Zhan BAI)**